From the Rolf Luft Research Center for Diabetes and Endocrinology,
Department of Molecular Medicine and Surgery,
Karolinska Institutet, Stockholm, Sweden

IN VIVO REGULATION OF PANCREATIC BETA CELL FUNCTION

Pim Pieter van Krieken

Karolinska Institutet

Stockholm 2018

Cover illustration by Liesbeth van Triest.

Published by Karolinska Institutet.
Printed by E-Print AB 2018.

ISBN 978-91-7676-923-2

IN VIVO REGULATION OF PANCREATIC BETA CELL FUNCTION

THESIS FOR A DOCTORAL DEGREE (Ph.D.)

BY

Pim P. van Krieken

Public defence on Friday the 23rd of March 2018 at 9:15 am
Lecture hall 'medicine', Karolinska University Hospital A6:04, Solna

Principal Supervisor:
Dr. Erwin Ilegems
Karolinska Institutet
Department of Molecular Medicine and Surgery

Co-supervisor:
Professor Per-Olof Berggren
Karolinska Institutet
Department of Molecular Medicine and Surgery

Opponent:
Professor Guy Rutter
Imperial College London
Department of Medicine

Examination Board:
Professor Per Uhlén
Karolinska Institutet
Department of Medical Biochemistry and Biophysics

Professor Per-Ola Carlsson
Uppsala University
Department of Medical Cell Biology

Professor Anna Krook
Karolinska Institutet
Department of Molecular Medicine and Surgery

“I have never tried that before, so I think I should definitely be able to do that.”

— Astrid Lindgren, Pippi Longstocking

To my family

ABSTRACT

Pancreatic beta cells within the islets of Langerhans contribute to the regulation of glucose homeostasis by secretion of insulin, a hormone that stimulates the uptake of glucose by liver, muscle and fat tissue. In response to variations in insulin demand, the beta cell population can adapt by (1) changing the total beta cell mass, and (2) modulating the functional capacity of individual beta cells. A failure of this mechanism will lead to disturbances in glucose homeostasis and the development of diabetes mellitus. A better understanding of the mechanisms underlying the regulation of a functional beta cell mass can help comprehend how diabetes develops and facilitate efforts to advance therapeutic strategies.

Since quite some research has been performed on the regulation of beta cell mass, this thesis focused on elucidating mechanisms behind the functional adaptation of beta cells. The first part of the thesis describes the development of several tools to be able to study the beta cells in the context of the islet *in vitro,* and *in vivo* following transplantation into the anterior chamber of the mouse eye (ACE). Exploiting confocal microscopy and the intrinsic light scattering properties of islet cells, a label-free methodology was developed to describe the morphology and secretory status of the islets. This approach was utilised to quantify the islet volume and study islet mass kinetics in different mouse models of diabetes. Taking advantage of pseudoislets, a novel procedure was established to genetically engineer islets pre-transplantation. It was shown that the synthetic modulation of an amplifying pathway in the beta cell could be used to regulate islet graft function, indicating that this technique is suitable to assess the role of specific proteins in beta cell function *in vivo*.

In the second part, we researched how murine beta cells naturally regulate their function *in vivo* using a model of reduced beta cell mass. First, pancreatic beta cells were removed, leading to hyperglycaemia. Subsequently, glycaemia was normalised by transplanting a minimal number of islets into the ACE. This model enabled us to study the consequences of an increased workload on beta cells. It was found that long-term exposure to high workload leads to several functional adaptations *in vivo* as well as changes in the islet gene expression profile, thus indicating that beta cells can display functional plasticity under normoglycaemic and non-obese conditions.

Our newly developed tools have broadened the possibilities to assess and enhance beta cell function *in vivo,* and helped to gain insights into the mechanisms regulating functional beta cell mass. Collectively, the technical advances and findings presented in this thesis could be used to improve diagnostics and therapeutics for diabetes.

LIST OF SCIENTIFIC PAPERS

This thesis is based on the following papers, which in the text will be referred to by their Roman numerals:

I. **Light scattering as an intrinsic indicator for pancreatic islet cell mass and secretion.**
Erwin Ilegems, Pim P. van Krieken, Patrick Karlsson Edlund, Andrea Dicker, Tomas Alanentalo, Maria Eriksson, Slavena Mandic, Ulf Ahlgren, Per-Olof Berggren.
Scientific Reports (2015) Jun 1;5:10740.

II. **Kinetics of functional beta cell mass decay in a diphtheria toxin receptor mouse model of diabetes.**
Pim P. van Krieken, Andrea Dicker, Maria Eriksson, Pedro L. Herrera, Ulf Ahlgren, Per-Olof Berggren, Erwin Ilegems.
Scientific Reports (2017) Sep 29;7:12440.

III. **A synthetic biology approach in the regulation of islet graft function.**
Pim P. van Krieken, Andrea Dicker, Anya Voznesenskaya, Jeong Ik Lee, Erwin Ilegems, Per-Olof Berggren.
Manuscript

IV. ***In vivo* functional adaptation of islets to a decrease in beta cell mass.**
Pim P. van Krieken, Andrea Dicker, Per-Olof Berggren, Erwin Ilegems.
Manuscript

Publications not included in this thesis:

- **Sequential intravital imaging reveals *in vivo* dynamics of pancreatic tissue transplanted under the kidney capsule in mice.**
Léon van Gurp, Cindy J. M. Loomans, Pim P. van Krieken, Gitanjali Dharmadhikari, Erik Jansen, Femke C. A. S. Ringnalda, Evelyne Beerling, Jacco van Rheenen, Eelco J. P. de Koning.
Diabetologia (2016) Nov;59(11):2387-2392.

- **Fabrication of three-dimensional bioplotted hydrogel scaffolds for islets of Langerhans transplantation.**
Giulia Marchioli, Léon van Gurp, Pim P. van Krieken, Dimitrios Stamatialis, Marten Engelse, Clemens A. van Blitterswijk, Marcel B. Karperien, Eelco J.P. de Koning, Jacqueline Alblas, Lorenzo Moroni, Aart A. van Apeldoorn.
Biofabrication (2015) May 28;7(2):025009.

CONTENTS

LIST OF ABBREVIATIONS

ACE	Anterior chamber of the eye
ANOVA	Analysis of variance
ATP	Adenosine triphosphate
AVP	[Arg^8]-vasopressin
$[Ca^{2+}]_i$	Intracellular free Ca^{2+} concentration
cAMP	Cyclic adenosine monophosphate
CLAHE	Contrast limited adaptive histogram equalisation
DMSO	Dimethyl sulfoxide
DNA or cDNA	(Complementary) deoxyribonucleic acid
DT or DTR	Diphtheria toxin (receptor)
EDTA	Ethylenediaminetetraacetic acid
ELISA	Enzyme-linked immunosorbent assay
ERK	Extracellular signal-regulated kinase
Fura-2/AM	Fura-2 acetoxymethyl ester
FAD	Flavin adenine dinucleotide
FoxM1	Forkhead box M1
GCK	Glucokinase
GFP	Green fluorescent protein
GLUT	Glucose transporter
GPCR	G-protein coupled receptor
GTT or ITT	Glucose or insulin tolerance test
HBSS	Hank's balanced salt solution
HFD	High fat diet
IP_3	Inositol 1,4,5-trisphosphate
K_{ATP} channel	ATP-sensitive potassium channel
LSM	Laser scanning microscopy
MODY	Maturity onset diabetes of the young
MRI	Magnetic resonance imaging
mTOR	Mechanistic target of rapamycin

NAD(P)H	Nicotinamide adenine dinucleotide (phosphate)
NeuroD (or Beta2)	Neurogenic differentiation protein
NOD	Non-obese diabetic
VEGF	Vascular endothelial growth factor
OCM	Optical coherence microscopy
OPT	Optical projection tomography
PBGD	Porphobilinogen deaminase
PBS	Phosphate-buffered saline
PDX-1	Pancreatic and duodenal homeobox 1
PET	Positron emission tomography
PFA	Paraformaldehyde
RIP / MIP	Rat or mouse insulin promotor
PKA	Protein kinase A
PKC	Protein kinase C
PLC	Phospholipase C
RNA	Ribonucleic acid
RT-PCR	Reverse transcription-polymerase chain reaction
SD or SEM	Standard deviation or standard error of the mean
SPECT	Single-photon emission computed tomography
STZ	Streptozotocin
Tx	Transplantation
T1D or T2D	Type 1 or 2 diabetes mellitus
TBST	Tris-buffered saline with Tween 20
TPEN	N,N,N',N'-tetrakis-(2 pyridylmethyl)ethylenediamine

1 INTRODUCTION

1.1 GLUCOSE HOMEOSTASIS

Maintaining a normal blood glucose homeostasis is essential for the function of all cells in our body and requires the interplay of several organ systems. Insulin and glucagon are the most important hormones to regulate blood glucose levels (glycaemia). The secretion of insulin and glucagon from the pancreas into the blood stream increases under relative hyperglycaemia and hypoglycaemia, respectively. Insulin stimulates the uptake of glucose by liver, muscle and fat tissue. Its function is counterbalanced by glucagon, which triggers the release of glucose from hepatic cells.

1.1.1 Pancreatic islets

The pancreas is a unique gland in the sense that it fulfils both an endocrine and an exocrine function. In mice, the gland can be subdivided into splenic, gastric and duodenal lobular compartments [1]. The majority of the pancreas consists of acinar cells that secrete digestive enzymes into the ducts leading towards the duodenum via the papilla of Vater. Only a small portion comprises of endocrine clusters called the islets of Langerhans or pancreatic islets. The islets have various sizes, ranging from 50 to 500 micrometres, and are found scattered throughout the pancreas (Figure 1). In the mouse pancreas, the larger islets seem to be arranged around the major blood vessels and ducts running from the splenic and gastric to duodenal lobe while smaller islets are mostly found in the periphery [2, 3].

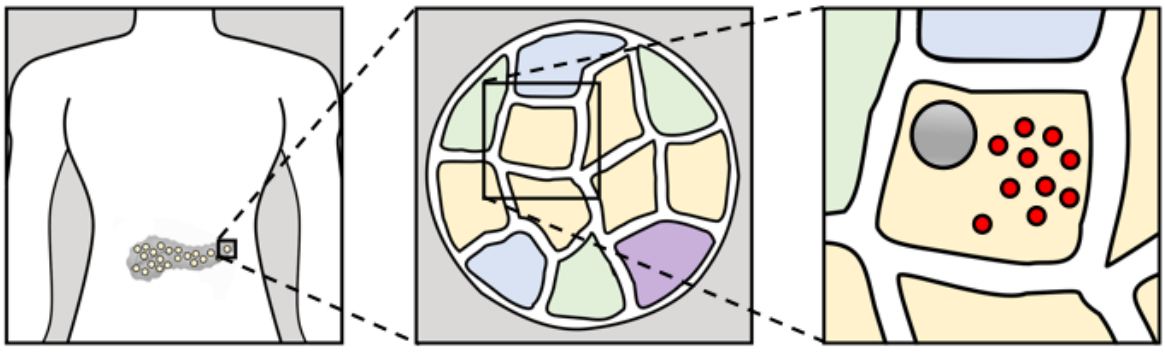

Figure 1: Anatomy of the pancreatic islet.

1.1.1.1 Islet cytoarchitecture

Within the islet typically five highly specialised hormone-producing cell types are found: About 20-40 percent comprises glucagon-producing alpha cells, somatostatin-producing delta cells, pancreatic polypeptide-producing PP-cells, and ghrelin-producing epsilon-cells. The remainder are beta cells, responsible for the production and secretion of insulin [4, 5].

Beta cells use paracrine signalling to communicate with the other endocrine cells found in the islet. Importantly, human and rodent islets have somewhat different paracrine signalling pathways related to their cellular composition [6, 7]. Whereas in human islets beta cells are intermingled with the other endocrine cell types, rodent islets typically have a mantle of alpha and delta cells and a core of beta cells. It is not completely understood to what extent this affects islet cell function [6]. Interestingly, pseudoislets formed by spontaneous reassembly of dispersed rat islet cells were observed to have the same mantle-core structure found in intact islets [8], suggesting that individual cells within the pseudoislet can maintain the paracrine signalling that exists in intact islets. Jointly, these findings indicate that beta cell studies should preferentially be performed within the context of the intact islet or pseudoislet.

1.1.1.2 Islet vascularisation and innervation

Islet cells get their oxygen, nutrients (e.g. glucose), and hormones such as incretins from the same blood vessels that supply the exocrine pancreas. However, islets receive 5-15% of all the pancreatic blood flow despite comprising only 1-3% of the total pancreatic volume [9]. The intra-islet blood flow is regulated by nervous input and, in the case of rodents, involves both sympathetic and parasympathetic nerves. In addition, intra-islet hormones, connexin36 and glucose levels have been shown to influence islet blood flow [10-13]. Interestingly, a recent report showed that blood flow is not affected by glucose concentrations in islets from non-human primates [14]. In mice, parasympathetic axons further influence beta cell function by secreting acetylcholine, a major neurotransmitter that acts on the muscarinic receptors of islet cells [15]. However, human islets have an innervation pattern consisting almost exclusively of sympathetic nerve fibres [16] and acetylcholine is instead produced by alpha cells [17]. Together, these studies demonstrate that islets require a dense network of vascularisation and innervation to facilitate a proper endocrine function.

1.1.2 The beta cell

Insulin is synthesised via its precursors preproinsulin and proinsulin, packaged as a hexamer with Ca^{2+} and Zn^{2+} ions, and stored in vesicles in the cytoplasm awaiting secretion [18]. The beta cell has a readily releasable pool of vesicles (1-5%) that provides an initial burst of secretion and can be followed by second phase insulin release of the subsequently recruited pool of secretory vesicles [19].

1.1.2.1 The role of the beta cell in glucose homeostasis

Between glucose sensing and insulin secretion a cascade of events occur known as the triggering pathway (Figure 2) [20]. Extracellular glucose enters the beta cell via glucose

transporters (predominantly GLUT1 in human, GLUT2 in mouse) and is rapidly metabolised by glycokinase to generate ATP and pyruvate. In the mitochondria, pyruvate is processed resulting in increased NAD(P)H levels and the production of more ATP. A rise in cytoplasmic ATP levels consequently closes ATP-sensitive K^+ channels (K_{ATP}), which leads to depolarisation of the cell membrane. In turn, this triggers the inflow of Ca^{2+} through voltage-dependent Ca^{2+} channels towards the cytoplasm. Additional Ca^{2+} is further mobilised from intracellular stores (i.e. the endoplasmic reticulum) mediated by inositol-1,4,5-trisphosphate (IP_3). The increase in $[Ca^{2+}]_i$ stimulates exocytosis of insulin-containing vesicles [20-22]. The intracellular free Ca^{2+} ($[Ca^{2+}]_i$) oscillatory pattern in the beta cell is associated with the pulsatile secretion of insulin into the blood stream [23-25].

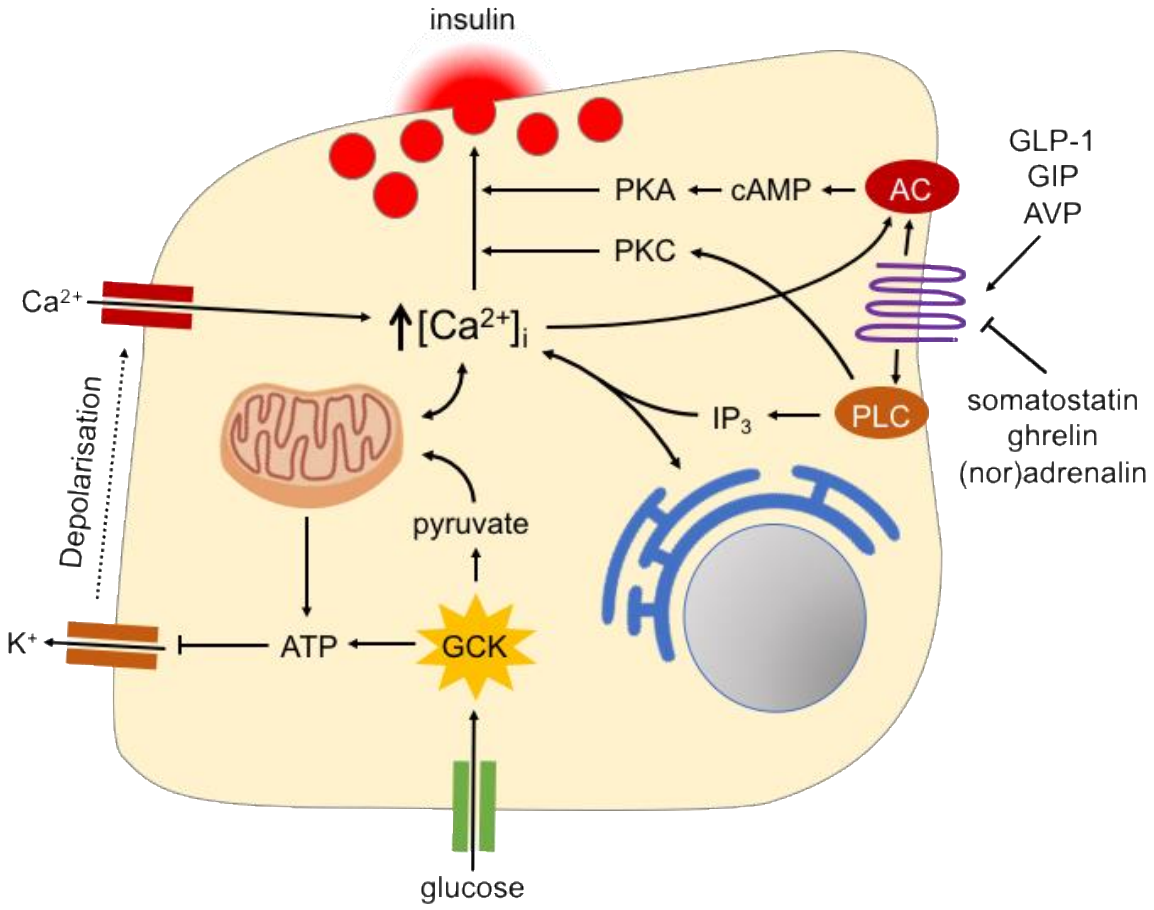

Figure 2: Intracellular signalling pathways in the pancreatic beta cell.

In addition to glucose, several other nutrients (i.e. amino acids, free fatty acids) and non-nutrient compounds (i.e. hormones and neurotransmitters) can modulate insulin secretion via G-protein coupled receptor (GPCR) amplifying pathways that affect the sensitivity of the secretory apparatus to $[Ca^{2+}]_i$ [20]. Activation of G_s- and G_q-coupled GPCRs stimulates insulin secretion respectively via cyclic adenosine monophosphate (cAMP) mediated activation of protein kinase A (PKA) or phospholipase C activation of protein kinase C

(PKC). Inversely, activation of G_i-coupled receptors leads to decreased sensitivity of the secretory machinery to $[Ca^{2+}]_i$ thus impeding insulin secretion [26].

Beta cells can function independently of their neighbours. However, studies on $[Ca^{2+}]_i$ demonstrate a high synchronicity between beta cells within the same islet, indicating that individual cells preferentially work as part of a secretory unit together with the other beta cells. This functional syncytium has been attributed to cell-to-cell coupling via gap junction proteins, e.g. connexin36 [27, 28] and recently proposed to be coordinated by specialised hub cells [29]. While a synchronised $[Ca^{2+}]_i$ pattern would suggest electrical coupling, non-synchronised oscillations could indicate a lack of electrically coupled beta cells. Indeed, single cells obtained from islet dispersion show altered basal insulin release patterns compared to intact islets [30]. It can be concluded that an adequate electrical coupling between individual beta cells is necessary for a proper first and second phase insulin secretion as well as an intraislet $[Ca^{2+}]_i$ synchronisation [27, 31].

1.2 DIABETES MELLITUS

1.2.1 Aetiology and epidemiology

Under normal conditions, fasting glycaemia in humans ranges between 4 and 6 mM (and between 6 and 8 mM in mice depending on the strain). Failure of beta cells to produce and secrete sufficient insulin for the maintenance of adequate glucose levels leads to the development of diabetes mellitus (hereafter shortened to diabetes). The majority of cases of diabetes fall into two broad aetiopathogenetic categories, namely type 1 (T1D) and type 2 diabetes (T2D). T2D comprises 90% of all cases while the other 10% is made up by T1D and less prevalent subtypes such as gestational diabetes [32]. Both T1D and T2D patients experience short- and long-term episodes of hyperglycaemia. Chronic hyperglycaemia can lead to microvascular and neural damage as well as kidney failure and other disorders [33].

The current prevalence of individuals with diabetes is estimated at 425 million worldwide, that is 8.8% of the population, and this number is expected to rise to 629 million (9.9%) in 2045 [32]. Due to its continuously rising incidence, diabetes has a significant social and economic impact on our society.

1.2.2 Clinical characteristics in humans and animal models

1.2.2.1 Type 1 diabetes

T1D is an autoimmune disorder that predominantly presents itself during childhood and is therefore also referred to as juvenile diabetes. Insulitis, i.e. the lymphocytic infiltration into

the islet, leads to a gradual beta cell destruction. Upon the emergence of hyperglycaemia, individuals may have already lost 40-85% of their beta cells depending on their age [34] whereas at later stages only a few percents are detected [35]. The prevalence of T1D varies dramatically between countries, strengthening the idea that the susceptibility depends on a certain genetic predisposition [36]. Although the role of genetics in the aetiology of T1D is important, an additional environmental trigger is thought to be required to initiate the process of insulitis [37, 38]. Over the past decades a large number of environmental factors have been found to be associated with the development of T1D, including several viruses [39] and changes in gut microbiota and permeability [40].

Animal models have been crucial in obtaining mechanistic data on the pathogenesis of diabetes [41]. The non-obese diabetic (NOD) mouse and the Biobreeding rat represent two of the most common models for T1D. These rodents spontaneously develop insulitis during the first few weeks after birth, often resulting in diabetes [42-44]. Chemical ablation of beta cells is another common method to induce a diabetic phenotype. It comes with the advantage that beta cell destruction can be initiated at any desired time point during the lifespan of the animal. For instance, administration of streptozotocin, a ligand of the glucose transporter, causes beta cell death in a dose-dependent fashion through alkylation and subsequent necrosis [45]. In addition, genetically modified mouse models can be used. For example, diphtheria toxin (DT) treatment of mice carrying the DT receptor on their beta cells enables selective beta cell destruction [46]. DT facilitates the inhibition of elongation factor 2, resulting in the inhibition of protein synthesis and ultimately cell death [47].

1.2.2.2 Type 2 diabetes

T2D is a complex and multifactorial disease that is often associated with obesity [48]. Many genetic mutations and environmental factors have been discovered to trigger diabetes as well as obesity. Impaired glucose tolerance due to decreased insulin sensitivity in tissues such as the liver, muscle and fat hallmarks the progression towards T2D. Human T2D subjects display an inability to rapidly release insulin after a meal, causing spikes in blood glucose values. To counter the decreased insulin sensitivity, beta cells hypersecrete insulin, progressively creating a hyperglycaemic and hyperinsulinaemic milieu [48, 49]. In long-standing T2D, factors including glucotoxicity and lipotoxicity lead to beta cell failure. The increased frequency of beta cell apoptosis observed in the pancreas of T2D subjects [50] explains why their beta cell number is, on average, found to be two-thirds less compared to healthy subjects [51, 52].

To mimic T2D phenotypes such as obesity and insulin resistance, researchers frequently use dietary models [53]. For instance, high-fat feeding is a practical means to increase calorie intake for a particular period of time and can be applied to rodents or other animal models. Alternatively, several rodent models exist that display chronic overeating due to a deficiency in leptin signalling: The ob/ob and db/db mice bear a mutation in the leptin protein and receptor, respectively [54, 55]. The Zucker Diabetic Fatty rat also has a mutation in the gene encoding for the leptin receptor [56]. An example of a non-obese yet glucose intolerant animal is the Goto-Kakizaki rat [57].

1.2.3 Clinical and experimental treatments

The goal of any diabetes treatment is not only to improve glucose homeostasis, but also to prevent or delay any possible complications that result from an imbalance in glycaemia. For the past century the substitution of insulin, either via subcutaneous injections or using an insulin pump, has been the primary choice of therapy for all individuals diagnosed with T1D. Alternatively, methods are being developed for oral, transdermal, intranasal, and inhalable administration of insulin [58]. Rather than only improving the lack of insulin (insulinocentric view), Unger and others have proposed a glucagonocentric view in which a dampening of the excess glucagon would decrease glucose release by the liver amongst other effects [59].

Although insulin supplementation is also common for individuals with T2D, the focus is often on dietary changes and lifestyle interventions. In addition, pharmacological treatments such as metformin, sulfonylureas and GLP-1 analogues are prescribed. The former decreases hepatic glucose release whereas the latter two enhance endogenous insulin secretion [60].

1.2.3.1 Beta cell regeneration and replacement strategies

Since no method of insulin delivery matches the capacity of the beta cells to maintain blood glucose levels within a strict range, several strategies are explored to replace the lost beta cells [61]. One option that is currently looked into is to regenerate existing beta cells, either through controlled proliferation or by reprogramming of exocrine and/or other islet cells into beta cells [62, 63].

Transplantation of the whole pancreas and of isolated pancreatic islets, obtained from deceased organ donors, have been successful in decreasing or sometimes even completely abolishing insulin dependence in T1D subjects [64, 65]. Despite the promising results, this option requires a life-time treatment with immunosuppressive drugs and is limited by the availability of donor organs [64]. The use of stem or progenitor cells would be a solution to

the limited supply of donor tissue. Significant scientific progress has recently been made in the field of stem cell transplantation [66] and the growth of new beta cells from progenitor cells [67].

1.2.3.2 Islet transplantation

The vast majority of islet transplantations performed in a clinical setting involve the intrahepatic infusion of islets via the portal vein. Because the liver may not provide the islets with the optimal conditions required for survival, multiple alternative sites have been evaluated in both experimental and clinical studies of islet transplantation [68, 69]. Considerations when selecting a transplantation site include the accessibility, survival of the graft, and drainage of the secreted insulin to the target organs. In most rodent studies, islets are transplanted beneath the renal capsule, where they form an aggregated islet cell pellet. Alternatively, islets can be transplanted in locations where they engraft as individual islets, such as intraportally into the liver [70] or into the anterior chamber of the eye (ACE) [71].

The isolation procedure disrupts the islet from vessels and nerves, connections that need to be re-established following transplantation during the engraftment process. Depending on the transplantation site, revascularisation of rodent islets is initiated 1-3 days and completed 2-4 weeks post-transplantation [70-72]. Longitudinal imaging of autologous islet grafts in the ACE of primates demonstrated that in this more human-like setting revascularisation is initiated within 4-10 days and completed circa 90 days following transplantation [14]. Furthermore, mouse islets transplanted into the ACE were found to be reinnervated within circa one month [15]. The revascularisation process involves the ingrowth of endothelial cells from the host as well as outgrowth of intra-islet endothelial cells, provided the islets are freshly isolated, and is mediated by vascular endothelial growth factors (VEGF) [73-75]. Vessel remodelling and maturation occur to ensure a dense and functional vascular network in the islet graft, similar to that of *in situ* islets [70].

Although little is known about the engraftment efficiency of clinically transplanted islets, reports on human islets infused into the liver or placed under the kidney capsule of nude mice indicate that 50-70% of the islets are lost in the post-transplantation period. Moreover, the vascular density in these human islet grafts is lower than in endogenous islets [76-78].

1.3 REGULATION OF BETA CELL MASS AND FUNCTION

Two frequently used parameters in diabetes research are beta cell mass and beta cell function. The term beta cell mass refers to the total amount of beta cells (number or volume) in the

organism. Although the exact definition of beta cell function is more elusive, this parameter commonly describes the capacity of individual cells to secrete insulin in response to a triggering signal. In a pathological context, the opposite term beta cell dysfunction is used. A complete lack of beta cell function is referred to as beta cell failure. In principle, a defect in any of the components required for glucose sensing and insulin secretion can lead to beta cell dysfunction or failure.

The collective term functional beta cell mass thus refers to the insulin producing cells within the organism that contribute to the regulation of glucose homeostasis. Figure 3 illustrates how a change in functional beta cell mass in an example of diabetes progression results in hyperglycaemia.

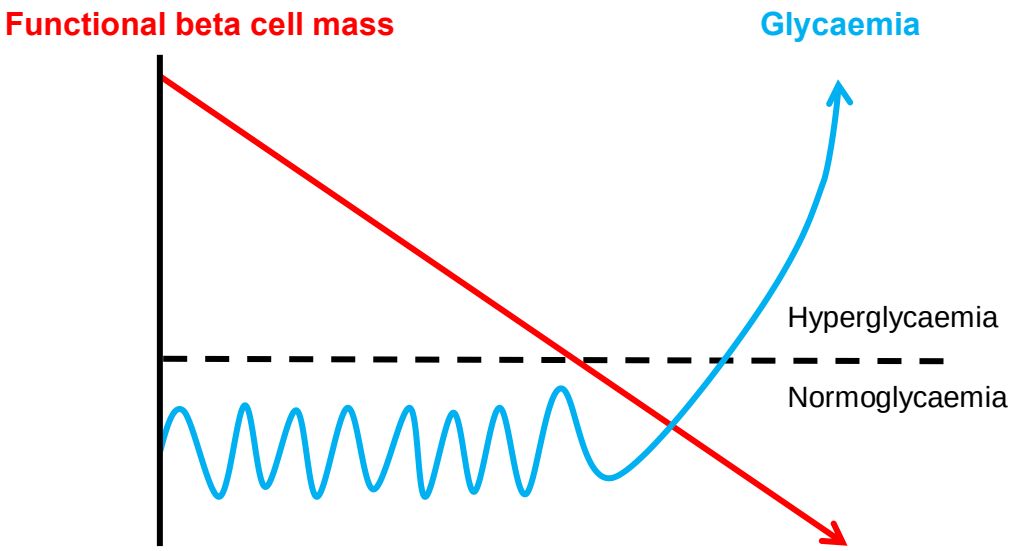

Figure 3: Relationship between functional beta cell mass and glucose homeostasis.

1.3.1 Regulation of beta cell mass

In mammals, beta cell mass is maintained by the careful balance of cell expansion and renewal (through replication or neogenesis), and cell loss (via apoptosis or autophagy) [79, 80]. Under normal physiological circumstances the rate of beta cell turnover and apoptosis are slow. An assessment of human beta cell replication pre- and postnatally indicates that proliferation is relatively high around the time of birth (0.5-5.0%) but remains low from six months onwards (0.1%) [81]. Similar or slightly higher numbers were found in rodents [82, 83]. Apoptosis that could occur during diabetes causes an imbalance that results in a shortage of beta cells.

Beta cell mass is dynamically regulated by certain physiological and pathophysiological cues related to changes in insulin demand [61, 84]. An adaptive beta cell mass expansion has been

found using rodent models of obesity and T2D [85-87], T1D [88], pregnancy [80] and beta cell loss or damage (e.g. partial pancreatectomy) [89-91]. Obesity was also associated with a higher beta cell turnover in human pancreas samples [92]. In contrast, no increased proliferation could be detected in the beta cells from individuals with T2D having impaired fasting glucose [92], recently diagnosed T1D patients [93] and subjects that previously underwent partial pancreatectomy [94]. It has been proposed that the proliferative capacity of the beta cell is to some extent restricted by age [95, 96]. Since most rodents studies are performed with relatively young animals, these results may not be comparable to the human pancreas [96, 97]. Moreover, neogenesis from non-endocrine pancreatic cells, and not proliferation, seems to be the dominant mechanism of adaptive beta cell growth in humans [98].

Glucose is thought to be the main cue involved in the regulation of beta cell mass. Systemic infusion of glucose markedly increased beta cell growth, while dampening glucose levels by insulin infusion had the opposite effect [99-101]. A recent study suggests that glucose is able to induce proliferation of beta cells via mTOR and ERK activation [102]. Other components essential for proliferation include glucokinase, K_{ATP} channels, Beta-arrestin-2, cyclin D2, FoxM1, Beta2/neuroD, PDX-1 and insulin receptor substrate 2 [101-105]. During pregnancy, lactogenic hormones can modulate the local levels of menin and serotonin to increase beta cell proliferation [106, 107].

1.3.2 Regulation of beta cell function

The regulation of beta cell function also occurs in a dynamic fashion. Individual beta cells can modulate their function in terms of insulin production/secretion or altered responsiveness during (patho)physiological conditions such as those described above [108]. For instance, the evolution of T1D may involve a period of remission during which patients require smaller doses of exogenous insulin owing to increased endogenous insulin secretion. This so called "honeymoon phase" is commonly presented a few months or years after diagnosis [109].

1.3.2.1 Beta cell heterogeneity

Studies on partial pancreatectomy and the pancreas of T1D subjects upon diagnosis show that a loss of up to ~80% of the total beta cell mass does not lead to hyperglycaemia [34, 90, 110, 111], indicating that rodents and humans have an enormous overcapacity in terms of functional beta cell mass. It further implies that beta cell function is heterogeneous [112], and that a certain proportion of islet cells has a low functional status (i.e. dormant or in a different stage of their life cycle) that could be triggered under higher demands.

Beta cell heterogeneity has been demonstrated from various angles including glucose-responsiveness, insulin promotor activity, insulin protein levels (reviewed in [113]), endoplasmic reticulum content, number of secretory granules, size of the beta cell nucleus (reviewed in [114]), overall beta cell size [115], insulin secretion [116], and Ca^{2+} oscillations [117]. Using electron microscopy it was shown that, compared to beta cells in the periphery of the rat islet, beta cells in the core are more degranulated after glucose stimulation [118]. The recent discoveries of several subpopulations of beta cells based on next generation sequencing experiments have confirmed the concept of a heterogeneous beta cell population [119-121].

Variations in function have not only been demonstrated between individual beta cells but also between individual islets within the pancreas after glucose stimulation [118] or high-fat diet (HFD) [122]. Differences in blood perfusion could be an underlying explanation of such beta cell heterogeneity [123].

1.3.2.2 Animal studies on functional beta cell adaptation

Not much is known about functional plasticity in human beta cells. Most of the current knowledge comes from studies on animals, predominantly rodent models of insulin resistance and obesity. Alternatively, models of pregnancy and decreased beta cell mass, e.g. partial pancreatectomy, have been explored. In the following section, the observations from some key animal studies are briefly discussed in order to obtain an overview of phenotypical changes naturally occurring in rodent beta cells.

In studies of HFD, mice gradually become obese. Gonzalez *et al.* [115] demonstrate that this does not only lead to compensatory beta cell proliferation, but also to functional adaptations. Using islets isolated from female mice fed a HFD for 12 weeks they found that beta cells displayed hypertrophy, contained more insulin and exhibited increased $[Ca^{2+}]_i$ signalling and insulin secretion upon glucose stimulation compared to beta cells from mice on control diet. In addition, islets from mice exposed to HFD contained a greater number of glucose responsive beta cells and, likely due to their increased size, the number of exocytotic events per beta cell was higher. In contrast, Chen and co-workers [124] could show an increased basal and blunted glucose-stimulated $[Ca^{2+}]_i$ amplitude in beta cells after 8 and 16 weeks of HFD using an *in vivo* microscopy approach. Moreover, in their model an increase in islet size could not be explained by beta cell hypertrophy. By repeated *in vivo* imaging of the same islet it was found that HFD feeding led to a transient degranulation and a minimal but significant widening of the intraislet vessel diameter.

Beta cells in obesity models such as the ob/ob and db/db mice also seem to display functional changes during the first weeks after birth. Islets isolated from the ob/ob and prediabetic db/db mouse were observed to have a higher insulin content due to augmented insulin biosynthesis, and increased glucose-induced insulin secretion [125-127]. Compared to controls, beta cells in these islets exhibited changes in their $[Ca^{2+}]_i$ pattern under relatively low glucose levels (<8.0 mM), suggestive of enhanced glucose sensitivity [125, 126]. Furthermore, in islets from ob/ob mice an improved Ca^{2+} mobilisation, increased mitochondrial activity [125], beta cell hypertrophy and blood vessel dilation were observed [86]. Yet, these alterations were paralleled by beta cell uncoupling and worsened glucose clearance *in vivo* [86, 125].

However, not all animal models of obesity/diabetes are suitable to investigate functional beta cell plasticity. In the Zucker fatty and Zucker diabetic rat models for example, some studies show functional compensatory mechanisms within islets such as hypersecretion of insulin and upregulated glucose metabolism [128, 129], while others only report changes in beta cell mass and not in function [130].

In studies of decreased beta cell mass an improvement in individual beta cell function could be observed. Islets remaining after 60% and 90% pancreatectomy outperformed control islets from sham-operated rats in terms of insulin secretion and glucose utilisation, and had a lower sensitivity threshold for glucose through a mechanism involving increased glycolytic activity and glucokinase levels [131-133].

Finally, changes in beta cell function are seen in the early stages of pregnancy. Islets isolated from pregnant mice or treated for 4 days with prolactin *in vitro* (to simulate pregnancy) exhibited a lower glucose sensitivity threshold, improved insulin secretion and beta cell coupling, islet cell hypertrophy and upregulated insulin biosynthesis [134-136].

Together, these studies indicate that rodent beta cells can exploit several adaptive mechanisms. It remains elusive how many independent mechanisms are involved in the regulation of a functional beta cell mass. It is conceivable that different (patho)physiological cues have their own pathways and are thus unrelated processes operating in parallel. To what extent the mechanisms found in rodents can be translated to human is an ongoing debate.

A better understanding of the adaptive mechanisms in the beta cell can (1) facilitate efforts to expand beta cells and enhance their functional capacity *in vitro*; (2) advance therapeutic options *in vivo*, e.g. the identification of small molecules to target beta cell specific pathways; and (3) help comprehend how diabetes develops due to a failure in these mechanisms.

1.4 IMAGING OF BETA CELL MASS AND FUNCTION

Beta cell mass and beta cell function are relevant biomarkers for the staging and diagnosis of diabetes, or to evaluate treatments [34, 137, 138]. Because the size of the beta cell population is controlled via a feedback loop that is directly coupled to its function, the two parameters are sometimes used to describe or predict each other [139-144].

1.4.1 *In vitro* and *ex vivo* methods to study beta cell mass and function

Historically, beta cell mass assessment has been limited to quantification of the pancreatic insulin content and insulin-labelled area in sliced pancreatic tissue. The development of optical projection tomography (OPT) for whole pancreatic samples for the first time provided stereological information to in depth describe islet distribution throughout the organ and analyse the total beta cell volume [145]. A clear drawback of these *ex vivo* approaches is that experimental assessment of beta cell mass kinetics required many animals.

Although repeated measurements of beta cell function can be performed *in vivo* (e.g. intravenous or oral glucose tolerance test and hyperglycaemic clamp), these only reflect the situation in the entire beta cell population and not individual cells or islets. Insulin release can however be studied from individual or groups of isolated islets or (beta) cells *in vitro*, but this will deprive them from their natural microenvironment and many circulating factors. Nevertheless, most of our current knowledge on islet function comes from studying isolated islets.

1.4.1.1 Fluorescent biosensors for imaging of islet function

A range of fluorescent biosensors has been developed to study several of the steps involved in glucose-induced insulin release [146]. As such, glucose uptake kinetics could be monitored by fluorescent glucose analogues [147]. Changes in $[Ca^{2+}]$ in various intracellular cell compartments were recorded by a number of fluorescent indicators and genetically encoded probes [148, 149]. Further, exocytotic events have been visualised using Zn^{2+} which is co-released with insulin or a pH-sensitive probe that reflects changes occurring upon granule fusion [150-152]. Of these, $[Ca^{2+}]_i$ has by far been the most commonly used read-out.

1.4.2 *In vivo* imaging of beta cell mass and function

Recent advances in the field of intravital imaging, such as the development of novel tracers as well as functional and molecular imaging methods, have opened new opportunities to study beta cell mass and function in a clinical or pre-clinical setting [138, 153]. Two broad

types of modalities can be distinguished to image the beta cell *in vivo*: optical and non-optical imaging.

Non-optical imaging modalities including magnetic resonance imaging (MRI), positron emission tomography (PET), and single-photon emission computed tomography (SPECT) are already available in a clinical setting and therefore represent the preferred screening platform for humans. While the research field has mainly focused on the quantification of beta cell mass, either in the pancreas or from transplanted islets, some possible functional compounds have been proposed as well. For instance, MRI enhanced manganese imaging has been used for studies of beta cell mass but since it accumulates in glucose-activated beta cells proportionally to the glucose concentration, it could also be used as a functional biomarker for MRI [154].

Optical imaging techniques such as bioluminescence imaging, confocal laser scanning microscopy (LSM) and optical coherence microscopy (OCM) have been employed in experimental settings for imaging of pancreatic beta cell mass [155-157] and blood flow [158, 159]. However, confocal LSM and OCM required laparotomy and exteriorisation of the pancreas due to the limited optical accessibility of the islets, hence hampering repeated assessment. Instead, body windows have been suggested as a possible solution [160, 161].

1.4.2.1 Imaging of islets transplanted into the anterior chamber of the eye

In 2008, a novel *in vivo* imaging platform was presented that combined islets transplanted into the anterior chamber of the mouse eye with LSM [71]. Ingeniously, the cornea was used as a natural body window to visualise islets engrafted onto the iris. As a result, the high resolution of confocal microscopy could be exploited to study cellular events within islet cells in the living mouse or rat. Importantly, it was shown that islet grafts in the ACE could directly report on the status of the endocrine pancreas [86].

During the last decade, the ACE platform has been exploited for a number of studies on beta cell mass and function, as recently reviewed [162]. For instance, the progressive growth of islets in the ob/ob mouse and the gradual destruction of islet cells in the NOD mouse could be monitored in detail [86, 163]. Furthermore, several parameters of islet function have been studied. For example, ratiometric imaging of NAD(P)H and FAD autofluorescence was used to detect increased mitochondrial metabolism [164] and high speed recording of the biosensor GCaMP3 in a single confocal plane was performed to show changes in the beta cell $[Ca^{2+}]_i$ pattern [124].

Intraocular imaging of islets is not limited to confocal LSM. In 2016, the group of Prof. Lasser successfully applied OCM to islets transplanted into the ACE and demonstrated the usefulness of this technique for label-free investigation of the dynamics of individual islet mass and vessel density as well as blood flow [159]. Also, Nord *et al.* used vibrational microspectroscopy for the imaging of biochemical compounds from islets in the ACE [165].

The ACE platform thus enables real-time monitoring of islet grafts in response to external stimuli (e.g. glucose) and assessment of the same islet over time in great detail, rendering it the perfect tool to study the dynamics of beta cell function.

2 AIMS

Exploiting the recent progress in the field of intravital imaging, the general aim of this thesis was to investigate how beta cell function is regulated *in vivo.*

The first part of this work focuses on the establishment of several tools to study beta cell function. The following aims are defined:

- Development of an imaging method to study beta cell mass and function *in vivo*
- Generation and characterisation of a mouse model of minimal beta cell mass
- Development of an *in vivo* approach to assess the role of specific genes for beta cell function

In the second part, the mouse model of minimal beta cell mass is exploited to accomplish the following aims:

- Investigation of changes in beta cell function *in vivo*
- Identification of genes involved in the natural regulation of beta cell function

3 MATERIALS AND METHODS

3.1 MATERIALS

All materials were from Sigma, unless specified otherwise.

3.1.1 Solutions and buffers

Buffered solution used for perifusion and batch incubation experiments contained 125 mM NaCl, 5.9 mM KCl, 2.6 mM $CaCl_2$, 1.2 mM $MgCl_2$, 25 mM HEPES (pH 7.4) and 0.1% bovine serum albumin (BSA). TBST contained 0.15 M NaCl, 0.1 M Tris pH 7.5, 0.1-0.3% Triton X-100. Blocking buffer was based on TBST or PBS supplemented with 10% goat serum and 0.01% sodium azide. Hank's balanced salt solution (HBSS) was buffered with HEPES (pH 7.4) and supplemented with 1 mg/ml Collagenase A or P for islet isolation, or instead 0.5% bovine serum albumin for washing and hand-picking. Islet cell lysis buffer contained DEPC-treated water (Thermo Fisher Scientific), 0.2% Triton-X and 5% RNAseOUT (Thermo Fisher Scientific).

3.1.2 Culture media

RPMI-1640 was supplemented with 2 mM L-Glutamine, 100 U/ml penicillin and 100 µg/ml streptomycin, and 10% fetal bovine serum. CMRL-1066 (ICN Biomedicals) was supplemented with 10 mM HEPES, 2 mM L-Glutamine, 0.25 mg/ml Fungizone, 50 mg/ml Gentamycin, 20 mg/ml Ciprofloxacin, 10 mM Nicotinamide and 10% fetal bovine serum.

3.1.3 Fixatives

Fresh paraformaldehyde (PFA) was prepared by dissolving 4 g in 90 ml dH_2O with a temperature of >65°C following the addition of 25 µl 5 M NaOH. The cooled-down mixture was supplemented with 10 ml of 10x PBS and filtered. For transmission electron microscopy, a fixative was used containing 2.5% glutaraldehyde + 1% paraformaldehyde in 0.1 M phosphate buffer (pH 7.4). Post-fixation was done with 2% osmium tetroxide in 0.1 M phosphate buffer (pH 7.4).

3.2 ANIMAL MODELS

All animals were housed in Karolinska Institutet's animal core facilities in a temperature (22 ± 2°C) and humidity controlled room with a 12-hour light/12-hour dark cycle. Animals had access to water and standard rodent chow diet. Animal experiments were performed in accordance with Karolinska Institutet's guidelines for care and use of animals in research and approved by the animal ethics committee at Karolinska Institutet.

C57BL/6J mice, SJL mice and Wistar rats were purchased from Charles River Laboratories (Germany). MIP-GFP mice, ob/ob ($Lep^{ob}/Lep^{\mathbf{ob}}$), and Ins-GCaMP3 mice were inbred at the animal core facility on a C57BL/6J background for at least 10 generations. RIP-DTR mice expressing diphtheria toxin receptors (DTR) on their beta cells [46] were kept on a mixed background or backcrossed one generation on a C57BL/6J background. MIP-GFP mice express green fluorescent protein (GFP) in their beta cells [166]. The ob/ob colony originates from Umeå, Sweden, and was shown to be insulin resistant between the age of 2 and 7 months [167]. Ins-GCaMP3 mice were generated by crossing heterozygous B6(Cg)-*Ins*$^{tm1.1(cre)Thor}$/J mice [168] and B6;129S-*Gt(Rosa)26Sor*$^{tm38(CAG\text{-}GCaMP3)Hze}$/J mice [169]. Ins-GCaMP3 mice express the genetically encoded Ca^{2+} sensitive biosensor GCaMP3 in their beta cells enabling fluctuations in $[Ca^{2+}]_i$ to be monitored by changes in fluorescence intensity [170].

3.3 METABOLIC TESTS AND TREATMENTS

3.3.1 Glucose and insulin measurements

Blood glucose concentrations in mice were obtained by measuring a drop of blood from the tail vein with a Accu-Chek Aviva system (Roche), which allows readings up to a maximum of 35.0 mM. Higher values were considered 35.0 mM. Plasma was obtained by collection of blood via the tail vein in EDTA coated micro-cuvettes following centrifugation at circa 1000 g for at least 10 minutes at 4°C. Plasma was stored at -20°C pending insulin content analysis with AlphaLISA (Perkin Elmer) according to the manufacturer's instructions in duplicate or triplicate. For pancreatic insulin content measurements, the pancreas was collected in ice cold PBS, weighed, transferred to 1.4 ml of ice cold acid ethanol (75% ethanol, 0.2 M HCl), homogenised with a handheld tissue homogeniser and stored at -20°C. On the day of analysis, a probe-sonicator was used for further cell lysis prior to measurement with ultrasensitive mouse insulin enzyme-linked assay (ELISA) kit (Crystal Chem Inc.) in duplicate.

3.3.2 Glucose and insulin tolerance tests

Prior to glucose and insulin tolerance test (GTT or ITT), animals were fasted overnight (12 hours), in the morning (6 hours) or used unfasted as indicated. For a GTT, mice received an intraperitoneal injection of 2 g glucose per kg bodyweight. For an ITT, mice received 0.5 U insulin per kg bodyweight by intraperitoneal injection. Glycemia was measured at fixed time points up to 150 minutes, as indicated.

3.3.3 Streptozotocin and diphtheria toxin treatments

Streptozotocin (STZ) was freshly dissolved in citric acid buffer (pH 4.5) and administered by a single intraperitoneal injection to male 8-10-week-old mice following 4-6 hours fasting.

Depending on the experiment, a dose between 150 and 250 mg per kg bodyweight was used. Diphtheria toxin (DT) was stored at -80°C at a stock concentration of 2 mg per ml dH_2O. Animals received 500 ng DT via a single intraperitoneal injection regardless of their body weight.

3.4 IMMUNOHISTOCHEMICAL AND STRUCTURAL ASSESSMENT

Antibodies were diluted in blocking buffer. Incubation steps for blocking and primary antibody staining were 1 hour for sections, 24 hours for islet grafts and 48 hours for whole pancreas specimens. Secondary antibodies incubation steps were overnight for sections and 24-48 hours for whole mounts.

3.4.1 Paraffin sections

Tissues were dissected and rinsed with PBS following fixation with formalin for 48 hours at room temperature. Dehydrated tissue was embedded in paraffin and sectioned at 5 µm thickness by a shared facility at Karolinska Institutet. Dewaxed, rehydrated tissues were stained with haematoxylin and eosin, or blocked and insulin-labelled with chicken anti-insulin (1:200 dilution, Abcam) followed by goat anti-chicken Alexa Fluor 488 (1:1,000 dilution, Invitrogen) or guinea pig anti-insulin (1:1,000 dilution, DAKO A0564, Agilent Technologies) followed by goat anti-guinea pig Alexa Fluor 488 (1:1,000 dilution, Thermo Fisher Scientific). Nuclei were stained upon mounting using ProLong Gold Antifade Reagent with DAPI (Invitrogen). Images were acquired using a BD Pathway 855 system (BD Biosciences).

3.4.2 Frozen sections and whole mounts

Tissues were dissected in PBS, fixed in 4% PFA on ice for 2-3 hours, rinsed in PBS and placed in 30% sucrose solution overnight. For frozen sections, tissues were embedded in Optimal Cutting Temperature compound and sliced at 10 µm thickness. After blocking, the following primary and secondary antibodies were used in 1:1,000 dilution on sections or whole mount grafts to label insulin, glucagon or StrepTag II: guinea pig anti-insulin (DAKO), mouse anti-glucagon antibodies (Sigma G2654), mouse anti-Strep-tag II (Qiagen), goat anti-guinea pig Alexa Fluor 488, and goat anti-mouse Alexa Fluor 594 or 633 (Thermo Fisher Scientific). Frozen sections were further mounted with ProLong Gold Antifade with DAPI. Images were acquired using a Leica SP5 system.

For optical projection tomography, connective tissue membranes and lymph nodes were removed. Fixed tissues were dehydrated (stepwise) to 100% MeOH, exposed to at least five

freeze/thaw cycles at -80°C to facilitate antibody penetration, and bleached overnight in a mixture of MeOH (Thermo Fisher Scientific), DMSO and 15% H_2O_2 at a 2:3:1 ratio to reduce endogenous tissue fluorescence. Tissues were rehydrated back to TBST (stepwise), blocked, and stained with anti-insulin primary antibody (1:500 dilution, DAKO) and a secondary goat anti-guinea pig Alexa Fluor 594 (1:500 dilution). Each pancreas was divided into a splenic, gastric and duodenal lobe, which were separately embedded in a filtered low-melting agarose gel. Samples were cleared by submersion in a 1:2 mixture of benzyl alcohol (Scharlab) and benzyl benzoate (Acros Organics), three washes in total. Samples were slowly rotated and sequentially excited at 488 and 594 nm to visualise anatomy and insulin positive signal, respectively (Figure 4). A series of 800 projection images was acquired with a Bioptonics 3001 OPT scanner (SkyScan). A video protocol is available [171].

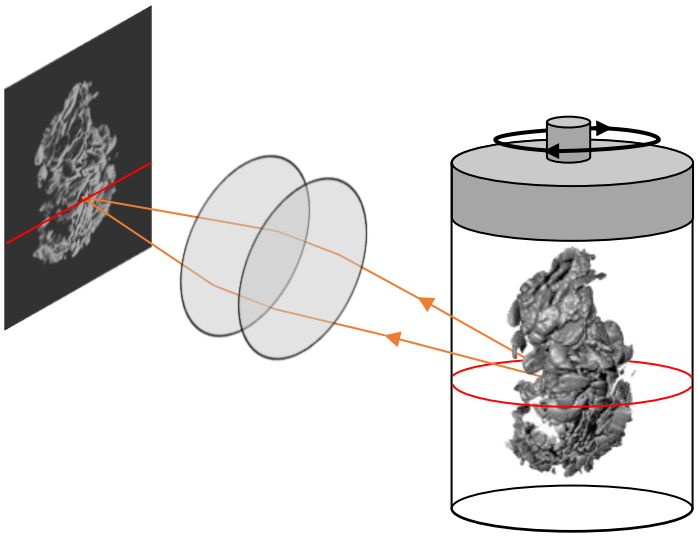

Figure 4: Schematic representation of a sample scanned by optical projection tomography. Adapted from Sharpe *et al.* [172].

3.4.3 Dead cells labelling

Islet cell death was assessed using an apoptosis kit (V13240, Invitrogen) following the manufacturer's instructions. Confocal images of dead cells within intact islets were acquired using a Leica SP5 confocal system.

3.4.4 Transmission electron microscopy

Small pieces of pancreas, isolated islets or whole islet grafts were pre-fixed at room temperature for 30 min and stored in fixative at 4°C. Subsequently, tissues were rinsed in 0.1 M phosphate buffer and post-fixed at 4 °C for two hours, dehydrated in ethanol followed by acetone and embedded in LX-112 (Ladd). Tissue processing, sectioning and transmission electron microscopy imaging were performed by the shared facility.

3.4.5 Zinc chelation and dithizone staining

Isolated islets were treated with 25 µM N,N,N',N'-tetrakis-(2 pyridylmethyl)ethylenediamine (TPEN) for 8 hours to remove intracellular Zn^{2+}. Treated islets were studied by reflected light imaging on a Leica SP5, stained with dithizone and imaged with a light microscope, or collected for transmission electron microscopy.

3.5 ISLET ISOLATION, PSEUDOISLET FORMATION AND TRANSDUCTION

3.5.1 Islet isolation

Mouse islets were obtained from both males and females aged between 2 and 8 months. Mice were sacrificed by cervical dislocation and sterilised with 70% ethanol. The abdominal organs were exposed by a V-section and the sternum and diaphragm were cut. The liver was tilted backwards and the intestines were placed outside of the abdominal cavity to expose the bile duct. The duodenal papilla was clamped with a bulldog clamp to prevent leakage into the duodenum. Next, the bile duct was cannulated with a 27-30 G needle attached to a polyethylene tubing and 2-3 ml of cold collagenase was slowly infused into the pancreas via the bile duct. If cannulation was unsuccessful the pancreas was cut in 1 mm^3 pieces. Excised tissue was placed in 2 ml additional collagenase solution. Enzymatic digestion was initiated by incubation at 37°C in a water bath and terminated by the addition of ice cold HBSS after 10-12 minutes. The digest was carefully disrupted using 18-22 G needles. Following three washes, islets were handpicked in non-adherent tissue culture dishes. Rat islets were prepared using similar methods. Islets were directly collected for RNA or protein extraction, or cultured in RPMI in a humidified atmosphere with 5% CO_2 at 37°C.

Human islets were obtained via the Nordic Network for Islet Transplantation, procured from deceased organ donors by established procedures [173], and cultured in CMRL.

3.5.2 Pseudoislet formation

Islets were dissociated into single cells by enzymatic digestion for 10 min at 37°C using Accutase followed by up and down pipetting to disrupt cell clusters. Cell numbers were determined using a TC20 automated cell counter (Bio-Rad). Droplets of 40 µl containing 62,500 cells per ml in cell culture medium were placed in each well of a 96-well GravityPLUS hanging drop system plate (Perkin Elmer). Pseudoislets were formed and collected after 6-7 days following the manufacturer's instructions.

3.5.3 Viral transduction

Islet cells were transduced with the adenoviruses RIP1-hV1BR, containing the coding sequence of the human V1b receptor together with a Strep-tag II label, and RIP1-R-GECO1, encoding for the red calcium indicator R-GECO1 [149]. Viruses were purified and concentrated using Fast-Trap (Millipore), following the manufacturer's instructions. Intact islets or a suspension of islet cells were transduced in the hanging droplet in the presence of 0.2, 1, 5 or 25 thousand viral particles per µl.

3.6 *IN VITRO* AND *EX VIVO* FUNCTIONAL EXPERIMENTS ON ISLETS

3.6.1 Measurements of intracellular Ca^{2+}

Intracellular free Ca^{2+} recordings were carried out with Fura-2/acetoxymethyl ester (Fura-2/AM) loaded islets that were either cultured overnight or freshly micro-dissected from the eye. Fura-2/AM is a ratiometric fluorescent Ca^{2+} indicator which is highly cell membrane permeable due to its lipophilic properties. Inside the cell, the cleavage of the acetoxymethyl ester traps Fura-2 inside the cytoplasm. Upon binding of Ca^{2+} to Fura-2, the molecule undergoes an absorption shift to shorter wavelengths. Alternating excitation between 340 and 380 nm allows the measurement of calcium bound and calcium free forms of Fura-2, respectively [174]. Islets were incubated for 1 hour with 2 µM Fura-2/AM in buffered solution with 3 mM glucose, mounted on a coverslip with Puramatrix Hydrogel (BD Biosystem), and perifused with various buffered solutions at 37°C. Perifusion buffer was supplemented with 3, 11 or 15 mM glucose, 25 mM KCl, and/or 100 nM [Arg^8]-vasopressin (AVP). Following excitation at 340 and 380 nm, fluorescence was collected using a 510/40 nm bandpass filter installed on an Axiovert 135 inverted epifluorescence microscope (Zeiss) connected to a Spex Industries Fluorolog system. Signals were normalised as described [175].

Islets transduced with R-GECO1 were starved for circa 30 minutes in a buffered solution containing 3 mM glucose, mounted in a Petri dish with Puramatrix Hydrogel and submerged in 2 ml of the buffer. Using a Leica SP5 system, confocal stacks were acquired every 15 seconds for ten minutes. After two minutes, 1 ml of buffered solution containing 39 mM glucose was added to reach a concentration of 15 mM glucose.

3.6.2 Static batch incubation

Groups of 8-12 cultured islets were incubated at 37°C in different buffered solutions for 30 minutes each. Following starvation (3 mM glucose), islets were incubated at low glucose (3 mM) and subsequently high glucose (11 or 15 mM). Buffers were collected for insulin concentration measurements with AlphaLISA. Islets were collected in M-PER protein

extraction reagent (Thermo Fisher Scientific) for analysis of insulin content with AlphaLISA and/or DNA content by Quant-IT Picogreen dsDNA kit (Thermo Fisher Scientific).

3.7 INTRAOCULAR TRANSPLANTATION OF ISLETS

Islet transplantation was performed as previously described [176]. In brief, the mouse was anesthetised with a mixture of isoflurane (Baxter) and oxygen, placed on a heating pad and restrained by fixation of the head in a custom-made head holder. Anaesthesia was delivered through a gas mask (Figure 5). The eye was immobilised with forceps and the cornea was punctured with a 23-25 G needle from the side. Islets were loaded in the tip of a glass cannula attached via a polyethylene tubing to a 1 ml Hamilton syringe. Following insertion of the tip of the cannula via the puncture site, islets were transplanted into the anterior chamber of the eye. Temgesic (0.1 mg/kg) was given subcutaneously for post-operative analgesia. Mice were observed until complete recovery. Overview images of transplanted eyes were obtained using a digital camera connected to a Leica M60 stereomicroscope.

3.8 FLUORESCENCE IMAGING OF ISLETS

3.8.1 Microscopy settings

Imaging was performed using a Leica TCS-SP2 or TCS-SP5 system equipped with Argon and HeNe lasers using 10x, 20x, 25x or 40x water-immersion objectives. Two-photon excitation was achieved using a Ti:Sapphire laser. Confocal stacks were acquired by reflection and fluorescence microscopy. While reflection microscopy is label-free, fluorescence microscopy requires fluorophores thereby allowing for the specific labelling of biological structures. Laser light is used to make optical sections in a plane of interest at a depth of up to a few hundred micrometres into the tissue at a subcellular resolution (<1 μm). The use of different laser lines for specific experiments is detailed in each paper. The step-size between each optical section was 2 or 4 μm. Images were generally acquired at 8-bit with a resolution of 512 x 512 pixels. Scanning speed and laser intensities were adjusted to avoid any cellular damage to islets *in vitro*, and to the mouse eye or islet grafts *in vivo*.

3.8.2 *In vivo* imaging of islets

For *in vivo* imaging (Figure 5), mice were anesthetised with isoflurane as described above. Viscotears was used as an immersion medium between the lens and the mouse eye. Islet grafts were imaged between 1 week and 5 months after transplantation. Blood vessels were visualised by intravenous injection of 2.5 mg/ml dextran labelled with FITC or Texas Red (500 or 70 kDa, Invitrogen).

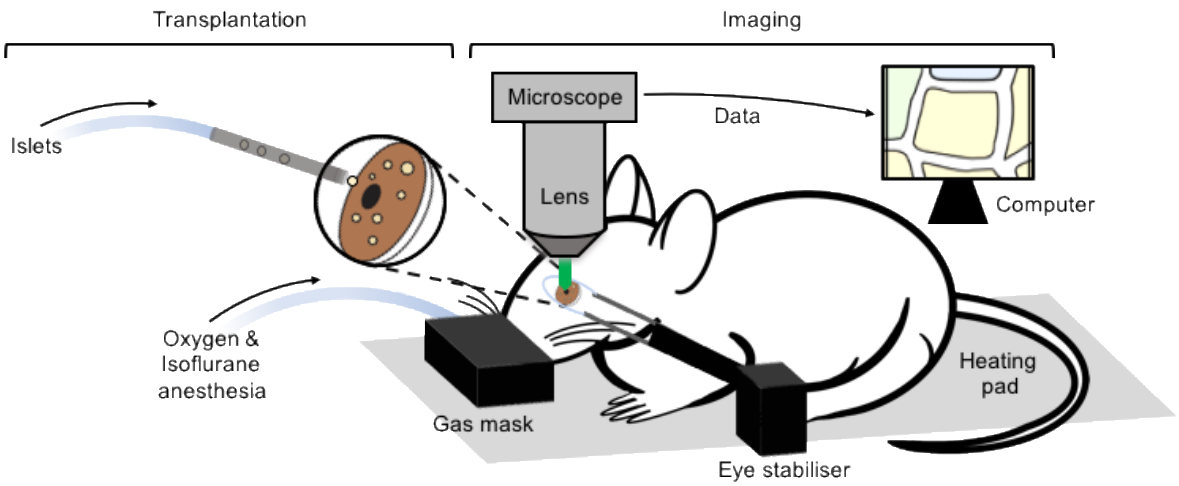

Figure 5: *In vivo* microscopy of islet grafts in the anterior chamber of the mouse eye.

3.8.3 NAD(P)H and FAD imaging

Nicotinamide adenine dinucleotide phosphate (NAD(P)H) and flavin adenine dinucleotide (FAD) are two endogenous fluorophores related to cellular metabolism occurring in the electron transport chain [177]. To image NAD(P)H and FAD, islet grafts were sequentially excited with a multiphoton laser at 760 nm and 900 nm, respectively. Signal was collected in a single plane at 12 bit with a resolution of 256 x 256 pixels using band-pass filters 460/50 and 525/50 and a resonance scanner at 8000 Hz.

3.8.4 *In vivo* intracellular Ca^{2+} imaging

Imaging of GCaMP3 islet grafts was performed with female (**Paper III**) or male mice (**Paper IV**). Males were fasted for 4 hours in the morning or 12 hours overnight and anesthetised by intraperitoneal injection of 8 or 6 µl of a midazolam/fentanyl mixture per g bodyweight, respectively. Females were anesthetised unfasted with 8 µl per g bodyweight. One part of premixed fentanyl citrate (0.315 mg/ml) and fluanisone (10 mg/ml, VetaPlasma) was freshly mixed with two parts water and one part midazolam (5 mg/ml, Hameln). A tail vein catheter connected to a tubing containing 100 U/ml heparin in saline was installed. Blood glucose was measured directly before and after the recordings. While a single islet graft was continuously excited with a fluorescent lamp, GCaMP3 fluorescence was collected at 16 bit with a Hamamatsu camera installed on top of a 35°C heated microscope chamber. During a 15 or 20-minutes recording, a piezo element under the control of LabVIEW software moved a 25x objective up and down every 2 s during which 60 images were collected, covering a xyz volume of 467 µm x 467 µm x 120 µm. After a 5-minute baseline a solution containing glucose (5%) or AVP (2 µM) was slowly (during 10 seconds) infused through the catheter at a dose of 4 µl per g bodyweight.

3.9 IMAGE ANALYSIS AND QUANTIFICATION

3.9.1 Optical projection tomography

Raw images obtained from optical projection tomography scanning underwent enhancement by applying a contrast limited adaptive histogram (CLAHE) algorithm with a 64 x 64 tile size as described before [178]. Tomographic reconstructions, made with NRecon v1.6.9.18 software (SkyScan), were loaded into Imaris 7.7.0 (Bitplane) for beta cell volume quantification. Islets, defined as clusters of insulin positive voxels, were obtained by a manually set threshold. Debris or artefacts and objects smaller than 20,000 μm^3 were removed, setting a detection threshold corresponding to spherical cell clusters of ~34 μm in diameter. Information on islet number and volume per pancreatic lobe was extracted.

3.9.2 Backscatter-based islet volume

AutoQuant X2 (Media Cybernetics) was used for deconvolution of confocal stacks acquired with the Leica SP2 system. No deconvolution was done for images acquired with the Leica SP5 system. Three different analysis protocols, each based on the backscatter signal, were used to quantify the volume of the islet graft. The islet volume in **Paper I** was calculated using Matlab (Mathworks) and defined as the equatorial volume which comprised backscatter positive signal from the top of the islet down to the equator. This script was found to work well for the analysis of islet growth over time. In **Paper II** the open source software Fiji [179] (version 1.50d or higher) was used to measure the projected area and perpendicular z-depth after applying the plugin Interactive Stack Rotation to line up the iris. Islet volume was calculated from the area and z-depth assuming the graft had the shape of half a sphere. This protocol was more accurate to quantify beta cell mass in shrinking islets. For **Paper IV**, the projected islet area was measured with Volocity and extrapolated to the volume of half a sphere. As demonstrated in **Paper I**, the projected area approximates the equatorial volume well and is a valid method to determine islet volumes when using large n-numbers.

3.9.3 Functional measurements

To analyse vessel volume and diameter, backscatter signal intensities, NAD(P)H/FAD ratio, beta cell size, and insulin or glucagon positive area, confocal images were loaded into Volocity (version 6.3, Perkin Elmer). Backscatter signal intensity was quantified for the whole islet (**Paper I**) or specifically in the beta cells of MIP-GFP islets exclusively using the signal that overlapped with the GFP signal while excluding dextran positive voxels (**Paper IV**). The only voxels included fell within a conical region of interest (ROI) with a diameter spanning 2/3 that of the islet and measuring 50 or 75 μm into the islet from the top towards

the centre. The obtained average intensity was normalised by dividing with the intensity of the iris around the islet. Vessel volume was obtained by manual thresholding of the dextran positive signal within the islet volume. An average islet blood vessel diameter was obtained by measuring the diameter (based on dextran positive signal in a maximum projection view) in three random blood vessels. The average beta cell size per islet was determined by manually measuring the area of 10 GFP positive cells per MIP-GFP islet. Insulin and glucagon positive area were determined by manual thresholding.

To analyse GCaMP3 recordings, Fiji software was used to obtain an average or maximum intensity projection for every two seconds of data. Each of the 450 or 600 time-frames was corrected for movement using the plug-in StackReg. The intensities over time were measured within the region of interest containing the islet.

3.9.4 Transduction efficiency and cell death

Transduction efficiency and islet cell apoptosis were determined as a percentage of the islet volume and calculated with Volocity. For each islet, the number of R-GECO1 or Annexin V Alexa Fluor 488 positive voxels was divided by the backscatter positive voxels by applying a manual threshold. Individual cells were automatically delineated within the R-GECO1 positive voxels by applying local contrast adjustment and thresholding for structures with a volume of approximately 1000-1500 μm^3.

3.10 RNA ISOLATION AND QUANTITATIVE RT-PCR ANALYSIS

Mouse iris containing single islet grafts was dissected in sterile ice-cold PBS. Using tweezers cleaned with RNaseZap (Thermo Fisher Scientific), a micro-biopsy was taken from single grafts and transferred to ice-cold lysis buffer. Biopsies were stored at -80°C until further processing using the Smart-seq2 protocol [180] to generate full length cDNA after RNA extraction. Quality of the obtained cDNA was verified using a High Sensitivity DNA Analysis Kit (Agilent Genomics) according to the manufacturer's instructions. Expression of all genes was measured by quantitative real-time PCR using SYBR green (Life Technologies) and a QuantStudio 5 system (Thermo Fisher Scientific). Genes were normalised to porphobilinogen deaminase (PBGD). Due to an insufficient amount of material, protein levels could not be assessed.

3.11 STATISTICAL ANALYSIS

Data was processed using Excel (Microsoft). Statistical analyses were performed with Prism version 6.0 (GraphPad Software) using student's unpaired and paired t-tests with a Holm-

Sidak post-hoc test when appropriate, Mann-Whitney tests or one-way ANOVA. Data is presented as mean ± SD or SEM, or as median ± interquartile range, depending on the data distribution. Statistical significance was considered for P-values <0.05. Figures were assembled using Prism and Photoshop (Adobe).

4 RESULTS AND DISCUSSION

4.1 DEVELOPMENT OF AN IMAGING METHOD TO STUDY BETA CELL MASS AND FUNCTION *IN VIVO*

To visualise islets or beta cells at high resolution, laser scanning microscopy is often combined with fluorescently labelled cells, for instance from the transgenic MIP-GFP mouse [71, 161, 181]. However, unlabelled endocrine tissues can also be detected based on their reflective properties [182, 183].

4.1.1 Reflected light imaging permits label-free visualisation of islet morphology and quantification of islet volumes over time

With reflected light microscopy, a beam of light is sent through an objective toward the islet, and photons that scatter backward at an angle of 180 degrees are collected via the same objective [184]. Reflected light imaging could be used to describe the 3D structure of islets isolated from mouse, rat and human using laser lines ranging from 458 nm up to 633 nm (**Paper I**, Figure 1), illustrating that islets exhibit similar reflective properties regardless of their origin or the wavelength used.

To test if the backscatter signal could also be used to obtain precise morphological data from islet grafts, we transplanted islets into the ACE and performed *in vivo* reflected light microscopy. Processing of the acquired confocal slices with a custom-made Matlab script allowed the quantification of (1) the area in a 2D projection view, and (2) the equatorial volume, i.e. the volume of the islet measured from the top down to the equator, in a 3D reconstruction (**Paper I**, Figure 2). A good correlation was found when data on the projected area and the equatorial volume from a large number of islets were plotted against each other (**Paper I**, Figure 3), thus suggesting that one parameter could be used to describe the other in this model of beta cell mass expansion. Additionally, repeated imaging of the same islet grafts over time allowed the study of beta cell mass dynamics.

To validate our islet mass analysis protocols, we turned to optical projection tomography (OPT) imaging, an established method to quantitatively assess beta cell mass *ex vivo* by exploiting whole-mount insulin staining and tissue clearing [145]. The same set of transplanted eyes was first imaged by reflected light microscopy and next collected and processed for OPT scanning. Accordingly, volumetric data was obtained from both modalities on the same islet grafts (**Paper I**, Figure 2). Although this data did not return the exact same volumes for individual grafts, likely due to changes in the *ex vivo* processing of

the samples, the ratios of single islet volumes were similar regardless of the imaging technique in use, validating backscatter intensity as a tool to accurately assess islet mass *in vivo*.

4.1.2 Reflected light imaging reports on the secretory status of the islet

As a side observation, longitudinal studies of ob/ob mice revealed that the development of insulin resistance was paralleled with a decrease backscatter signal in islet grafts [86]. Since the reason for this observation remained elusive, we decided to further investigate the light scattering properties of pancreatic islets. High resolution backscatter imaging illustrated that the punctate backscatter signal could be evenly detected in the cytoplasm of cells within the islet, but not in the nucleus (**Paper I**, Figure 1). Moreover, islets from hyperglycaemic mice were found to have significantly lower backscatter signal and insulin content (**Paper I**, Figure 4). Together, these observations indicated that the source of reflection is housed within the cytoplasm at a high concentration but reduced in a milieu of insulin hypersecretion.

It was hypothesised that the dense-core secretory granules within the beta cells (200-400 nm in diameter) were the main particles responsible for the strong light reflection based on the principle of Mie scattering, a phenomenon that applies to situations in which the size of the scattering particle is in the same range as the wavelength of light [185]. The hypothesis was tested by interfering with the formation of insulin crystals, a process that requires Zn^{2+} [18]. Indeed, treatment of islets with the Zn^{2+} chelator TPEN impeded insulin crystal formation as shown by electron microscopy. Furthermore, TPEN treated islets were found to have a decreased backscatter signal and lower uptake of the zinc-insulin crystal binding compound dithizone (**Paper I**, Figure 4). Although no direct changes in backscatter intensity could be monitored, our experiments demonstrate that the signal can be used as an intrinsic indicator for beta cell secretion *in vitro* and *in vivo*.

4.2 GENERATION AND CHARACTERISATION OF A MOUSE MODEL OF MINIMAL BETA CELL MASS

Changes in beta cell mass are a common feature in diabetes [186-188]. *In vivo* reflected light imaging was previously employed to monitor islet mass dynamics in models of obesity [86] and immune-mediated beta cell/islet destruction [163, 189]. However, despite being used extensively in diabetes research, surprisingly little data is available on the destruction kinetics of beta cell ablation models. To improve our understanding of the changes in beta cell mass in such models, we explored ablation mediated by diphtheria toxin (DT) and streptozotocin (STZ).

4.2.1 Loss in islet function precedes loss in islet mass in the RIP-DTR mouse model

DT administered to RIP-DTR mice was previously shown to induce near-total beta cell ablation within two weeks, leading to the conversion of alpha cells into beta cells in the period thereafter [46]. Following a similar protocol, we treated RIP-DTR mice with DT and collected the pancreas after 15 days for OPT. Subsequent quantification showed that DT treated mice had lost ~90% of their pancreatic beta cell mass compared to vehicle treated controls (**Paper II**, Figure 1 and supplementary movie). To study the day-to-day kinetics of beta cell destruction in these mice, RIP-DTR islets were transplanted into the ACE and monitored longitudinally by reflected light microscopy. Whilst no changes could be observed in the control islets, RIP-DTR islet mass rapidly decreased after treatment with DT. The loss of beta cell mass found in the ACE after 15 days was similar to that observed in the pancreas by OPT (**Paper II**, Figure 2), thus confirming previous observations [86] that islets in the eye report on the status of islets in the pancreas. Moreover, the amount of mass that remained at 4 days post-DT was in line with previous findings in which the beta cell mass of the RIP-DTR mouse was imaged using a bioluminescence approach [190].

The gradual beta cell death, which was preceded by a robust inhibition of protein synthesis [191], led to a sharp rise in glycaemia between day two and three post-DT and was paralleled by a decrease in circulating insulin levels. Prior to the emergence of hyperglycaemia, around 40 hours after treatment, RIP-DTR mice already presented impaired glucose intolerance (**Paper II**, Figure 3). At this point in time, when almost half the beta cell mass was lost, the remaining islet mass did not show any apparent morphological or ultrastructural changes although the insulin staining in the pancreas of RIP-DTR was found to be less homogeneous compared to controls (**Paper II**, Figure 4). The latter could be indicative of alterations in protein expression levels or insulin secretion. Intracellular Ca^{2+} experiments with isolated RIP-DTR islets as early as one day post-DT demonstrated functional defects in spite of a relatively intact morphology and insulin content (**Paper II**, Figure 5). These observations illustrate that in the RIP-DTR mouse islet function is lost prior to a substantial loss in islet mass.

4.2.2 Streptozotocin treatment induced rapid hyperglycaemia and near total loss of pancreatic insulin content

In a second model, beta cell loss was accomplished through the treatment with a single high dose of STZ. Repeated reflected light imaging of previously transplanted C57BL/6J mice illustrated a progressive decrease in islet mass upon STZ treatment (Figure 6), reminiscent

of the destruction kinetics seen in the RIP-DTR mice. Compared to DT treatment in RIP-DTR mice, STZ caused a more abrupt hyperglycaemia in C57BL/6J mice, generally within hours (**Paper III**, Figure 2; **Paper IV**, Figure 1), underlining the different mechanism of action of the two toxins [45, 47]. One month after STZ treatment the pancreatic insulin content was almost negligible.

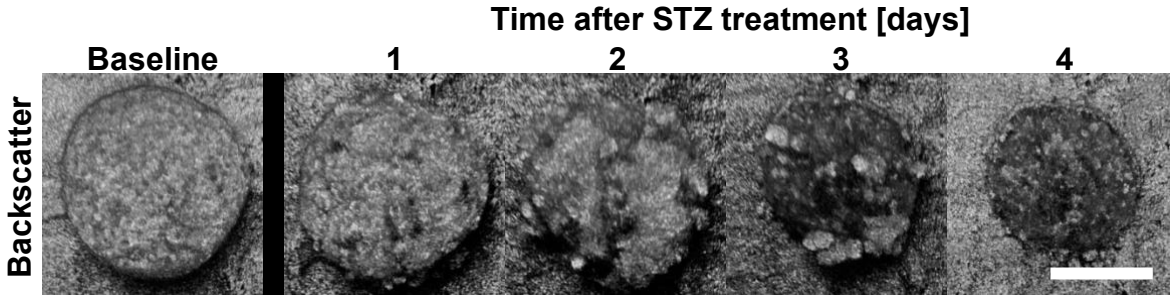

Figure 6: Confocal images obtained from *in vivo* microscopy show an engrafted islet shrinking over time after streptozotocin treatment. Scale bar represents 100 µm.

4.2.3 Combination of pancreatic beta cell ablation and islet transplantation creates a non-obese normoglycaemic model of minimal beta cell mass

The studies on beta cell destruction kinetics in these two mouse models prompted us to investigate how much functional beta cell mass is minimally required to maintain normoglycaemia. Namely, it was postulated that a minimal number of beta cells would increase the workload on the individual beta cell. In our hands, titration experiments demonstrated that the intraocular "metabolic" transplantation of at least 75-100 islets was needed to revert hyperglycaemia in two-month-old STZ-treated C57BL/6J mice (hereafter referred to as the STZ + Tx model; **Paper IV**, Figure 1). However, recovery of hyperglycaemic RIP-DTR mice of approximately 5 months of age required a transplantation of 100-150 islets. Several factors can be designated to influence the number of islets needed for normalisation of glycaemia, including the quality and average size of donor islets, the age of the recipient, and the beta cell mass remaining *in situ*.

Data on glycaemia, glucose tolerance and islet vascularisation obtained from the STZ + Tx model over time corroborated that engraftment was completed four weeks after the metabolic transplantation (**Paper IV**, Figures 1 and 2). Previous enucleation experiments performed after complete recovery immediately reverted hyperglycaemia [71], suggesting that the glucose homeostasis is maintained solely by the transplanted tissue. Furthermore, mice with a decreased beta cell mass were still able to efficiently handle a bolus of glucose despite lower circulating insulin levels, which could be explained by improved insulin sensitivity in

peripheral tissues (**Paper IV**, Figure 3). Thus, through pancreatic beta cell ablation with either STZ or DT and a subsequent metabolic transplantation of a minimal number of islets, two normoglycaemic and non-obese mouse models of decreased beta cell mass were established.

4.3 DEVELOPMENT OF AN *IN VIVO* APPROACH TO ASSESS THE ROLE OF SPECIFIC GENES FOR BETA CELL FUNCTION

To test the role of genes potentially involved in islet function, a beta cell specific expression methodology was developed. As a proof-of-concept we overexpressed the V1b receptor, a GPCR that is part of the vasopressin-oxytocin family and naturally expressed by beta cells at low levels [192, 193]. The choice for this receptor is twofold: Stimulation of the V1b receptor with its natural ligand AVP should elicit a direct mobilisation of $[Ca^{2+}]_i$ in beta cells via the PLC pathway. Concomitantly, *in vivo* administration of AVP would lead to a transient increase in glycaemia due to vasopressin receptor mediated gluconeogenesis in the liver, thereby enabling us to test if our modified beta cells still maintained a proper glucose-responsiveness.

4.3.1 Improved virus-mediated gene transfer using pseudoislets

To facilitate optimal gene transfer to all beta cells within the islets, we established a protocol in which dispersed islet cells in the presence of a virus were progressively reaggregated into pseudoislets, based on a previously pioneered method [194]. It was first confirmed that untransduced pseudoislets are functional *in vitro* and *in vivo* following transplantation into the ACE (**Paper III**, Figures 1 and 2). This is relevant as the pseudoislet formation requires temporary disruption of cell-cell contacts that are necessary for a proper islet function [7, 8, 30, 195]. Our protocol proved superior to transduction of intact islets and could even be used to transduce human islet cells (**Paper III**, Supplementary Figures 3 and 4). While it exposed the cells to the virus for a relatively long period, substantially lower virus titres could be used thus benefitting cell survival (**Paper III**, Figure 3).

4.3.2 Modulation of beta cell function by targeted overexpression of a GPCR

To be able to monitor islet function *in vivo* we engineered pseudoislets from GCaMP3 islet cells. We overexpressed the V1b receptor specifically in beta cells, transplanted the islets into the ACE and monitored fluctuations in $[Ca^{2+}]_i$ by real time fluorescent microscopy. As hypothesised, *in vivo* stimulation of pseudoislets with AVP acutely increased $[Ca^{2+}]_i$ in beta cells (**Paper III**, Figure 5). These results demonstrate that our expression methodology can be used to successfully modulate beta cell function by artificially modifying intracellular

pathways. Additionally, intravenous administration of AVP led to a gradual rise in glycaemia and consequently a secondary increase in $[Ca^{2+}]_i$ in beta cells, indicating that their glucose sensing mechanism remained intact. The current imaging protocol, just like a recently published setup by Chen and co-workers [124], enables the monitoring of changes in beta cell function *in vivo*. However, whereas their protocol is limited to single plane scanning, our protocol comes with the advantage that it uses GCaMP3 signal from the whole islet. Furthermore, the proof-of-concept experiments regarding the overexpression of the V1b receptor illustrate how our approach can be exploited to assess the role of specific genes for beta cell function.

4.4 INVESTIGATION OF CHANGES IN BETA CELL FUNCTION *IN VIVO*

Beta cells possess a natural ability to adapt their functional capacity [79]. To study the process of beta cell plasticity, we and others have recently utilised mouse models of obesity and insulin resistance [86, 115, 124, 126]. These mice have augmented circulating glucose and free fatty acid levels, both known regulators of islet function [196], making it difficult to identify other factors and pathways which can independently regulate beta cell function. To circumvent this and study adaptations in beta cells under normoglycaemic and non-obese circumstances, we employed our previously developed STZ + Tx model. These mice, and controls with an intact endocrine pancreas, received 5-10 reporter islets in their ACE (**Paper IV**, Figure 1).

4.4.1 Decrease in overall beta cell mass increases beta cell workload

To verify that we could increase the functional capacity of individual beta cells by decreasing the total amount of beta cells, we combined the information of several parameters. Based on measurements of beta cell mass decay and pancreatic insulin content, as well as the volumetric analysis of a graft consisting of 75-100 islets, it was estimated that STZ + Tx mice had a total beta cell mass comprising 20-50% the mass of controls. However, their circulating insulin levels were approximately one-thirds lower (**Paper IV**, Figure 3). Hence, it could be expected that the beta cells in the STZ + Tx model were pressured to perform at their maximal capacity to maintain normoglycaemia. Indeed, individual beta cells exhibited a transiently decreased light scattering phenotype suggestive of insulin hypersecretion, thus confirming an increased workload.

4.4.2 Increased insulin demand accelerates islet engraftment and causes beta cell hypertrophy

To study the effect of an increased beta cell workload on the engraftment process, islets were imaged at 1, 2 and 4 weeks after transplantation. Surprisingly, while the islets comprised the same range of sizes upon transplantation, quantification of their islet volume one week later showed that islets under high workload were significantly larger than islets transplanted in control mice. The increase in intraislet vessel volume, vessel diameter and the beta cell size found in islets in the high workload group could explain this difference (**Paper IV**, Figure 2). Beta cell hypertrophy has also been found in other conditions of high workload [86, 115, 136]. Although all islets are completely revascularised after four weeks, data from week 1 and 2 post-transplantation suggests that engraftment is accelerated in islets under high insulin demand. To our knowledge, no other studies have observed (or studied) differences in revascularisation under similar circumstances. However, similar studies investigating islets transplanted under hyperglycaemic conditions and in different locations did not detect any changes in revascularisation speed [197, 198].

4.4.3 Beta cells under high workload display functional adaptations *in vivo*

Beta cells were characterised in more detail after one month of exposure to high workload, when islet engraftment was completed. *In vivo* $[Ca^{2+}]_i$ recordings using Ins-GCaMP3 islets and NAD(P)H/FAD imaging suggested that beta cell metabolism was higher under basal conditions (**Paper IV**, Figure 4). This is in line with observations using HFD fed animals [124, 164]. In addition, while high glucose stimulation did not produce any differences in the amplitude of the $[Ca^{2+}]_i$ response, the timing of response was faster in islets that had been exposed to high workload compared to controls (**Paper IV**, Figure 4). The former result demonstrates that in our *in vivo* model beta cells remain functional after long-term exposure to high workload and do not precipitate failure within this time span. The latter finding, in combination with the lower glycaemia after 6 hours fasting (**Paper IV**, Figure 3), suggests a left-shifted or steeper sigmoidal curve with regards to glucose sensitivity and lowering of the glucose threshold. Hypersensitivity for glucose appears to be a common adaptive mechanism of beta cells in response to high workload as it was observed in several animal models [110, 125, 132, 135] including a similar STZ + Tx model [199].

4.5 IDENTIFICATION OF GENES INVOLVED IN THE NATURAL REGULATION OF BETA CELL FUNCTION

In pursuit of a mechanism that could explain the changes in beta cell function, we established a method that enabled gene expression analysis in single islet grafts. Our protocol was based

on a recently developed procedure for single cells [180] and involved the collection of RNA from an islet microbiopsy followed by the preparation of cDNA (**Paper IV**, Figure 5). Accordingly, we could compare differences in gene expression levels between individual grafts. Importantly, islet cells were spared from enzymatic digestion, yet an extra step that may affect the outcome in an already precarious procedure [200].

4.5.1 Upregulation of glucokinase is a natural adaptive response to improve beta cell function

In our preliminary analysis, while no differences were detected in the levels of insulin or glucose transporters, a twofold upregulation in glucokinase (GCK) mRNA was found in islets exposed to a month of high workload compared to control grafts (**Paper IV**, Figure 5). It is likely that the higher mRNA levels would translate into increased GCK activity, although this was not assessed at this stage. Since the processing of glucose by the GCK enzyme is thought to be a rate-limiting step in beta cell metabolism [201], this result is in agreement with our hypothesis that beta cells under high workload increase their functional capacity. In line with our results, two other studies found enhanced GCK activity in the islets of rats after partial pancreatectomy [131, 133]. Furthermore, mutations in the GCK gene (e.g. MODY2) result in various diabetic phenotypes in human subjects [202]. The current findings underpin the importance of GCK in the maintenance of a functional beta cell mass.

5 CONCLUSIONS AND OUTLOOK

The adaptive capacity of the beta cell is of paramount importance for the maintenance of a normal blood glucose homeostasis. Although quite some research has focused on the mechanisms behind compensatory beta cell expansion, our knowledge about the regulation of beta cell function remains poor, likely due to technical limitations. In this thesis work, we overcame some of these limitations through the development of several technical innovations, thereby allowing us to shed new light on the mechanisms underlying functional beta cell plasticity. The outcomes are graphically summarised in Figure 7.

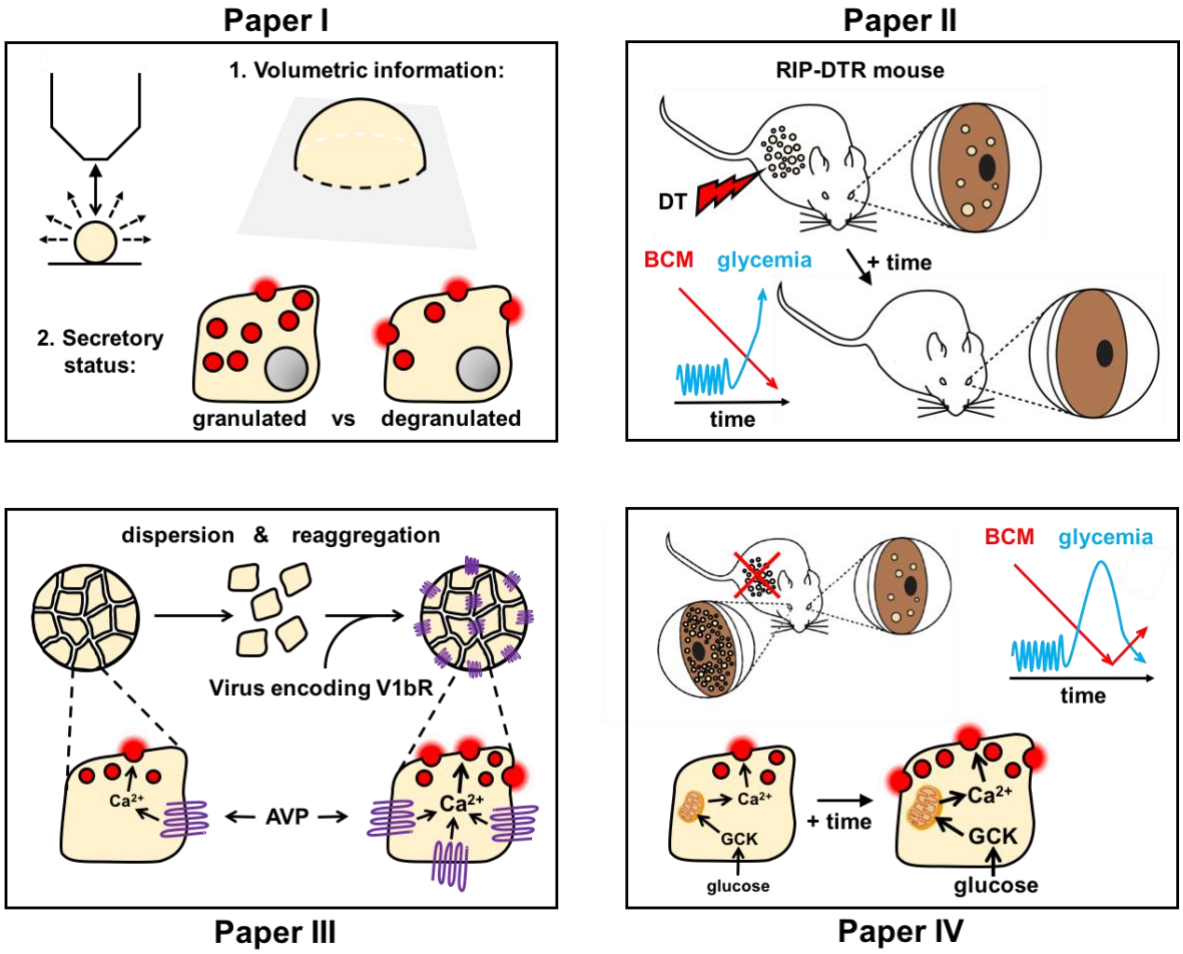

Figure 7: Graphical abstract of the papers included in this thesis.

We established a label-free method to non-invasively study changes in beta cell mass and function in the same islet over time by performing reflected light microscopy of endocrine tissues transplanted into the anterior chamber of the mouse eye. We developed analysis protocols that used the backscattered light signal to precisely quantify the volume and secretory status of single islet grafts (**Paper I**). Implementing our imaging approach allowed us to, for the first time, describe in detail the morphological changes in islets mass kinetics

in two commonly used mouse models of beta cell loss, the RIP-DTR mouse (**Paper II**) and the STZ-treatment model. Our findings from the combined measurements of islet mass and beta cell function illustrate that for accurate staging and diagnosis of diabetes it is of importance to monitor both parameters. During the last years, several research groups and consortia have attempted to broaden the possibilities to non-invasively image beta cells in a (pre-)clinical setting [138, 203]. Although our confocal microscopy-based approach to visualise beta cells *in vivo* has some inherent limitations e.g. owing to the poor tissue penetration, its application for humans is not unthinkable. Recently, Diez and colleagues modified the ACE platform for rodents and successfully imaged autologous islet grafts in the ACE of non-human primates [14].

We generated a mouse model of minimal beta cell mass through a combination of pancreatic beta cells ablation and a metabolic transplantation into the ACE (**Paper IV**). In conjunction with other observations [204], the results presented in this thesis demonstrate that relatively few islets are needed to re-establish a normal glucose homeostasis in mice. Hence, it is not necessary to replenish the initial beta cell mass completely. If this also holds true for human subjects is unclear. Most individuals can undergo partial (<50%) pancreatectomy without detrimental consequences for their blood glucose homeostasis [205], suggesting that humans, like rodents, also have some overcapacity regarding their functional beta cell mass. Yet, the "Edmonton protocol" prescribes the transplantation of at least 11,000 islet equivalents per kg into the portal vein to treat T1D individuals [65]. Such high numbers may not be required in a more islet-friendly transplantation site like the ACE, where the tissue is not hampered by for example immediate blood-mediated immune reactions. In line with this, it could be envisioned that the anterior segment of the human eye, despite harbouring limited space for islets, remains a feasible transplantation site for clinical islet transplantations.

We developed an approach to test the role of specific proteins in the regulation of beta cell function. As a proof-of-concept, we synthetically overexpressed a particular GPCR and could subsequently regulate islet graft function through stimulation of an amplifying pathway in beta cells (**Paper III**). Although the activation of specific GPCRs on the beta cell is a common pharmacological approach for T2D [26], it has been shown that GPCR expression decreases under diabetic conditions [206, 207]. Our beta cell specific expression methodology can, perhaps in combination with more stable viruses and a synthetically designed GPCR such as described by Guettier *et al.* [208], be used as a novel approach in the regulation of islet graft function.

We could increase the workload of individual beta cells by decreasing the overall beta cell mass. Islets transplanted under high workload conditions engrafted faster in terms of revascularisation. Moreover, their beta cells underwent several functional changes over the course of one month such as hypertrophy, hypersecretion of insulin, and hypersensitivity to glucose. It was concluded that mouse beta cells can display functional plasticity under non-obese and normoglycaemic circumstances. Our preliminary data suggests that the upregulation of GCK levels and/or activity is a natural adaptive response of beta cells to improve their function (**Paper IV**). As such, our findings in mice help to explain the phenotype of humans with mutations in the GCK gene (i.e. MODY2). Furthermore, in line with previous research, our results suggest that GCK is a potential target for future diabetes therapies. One approach that has gained momentum over the past few years is to pharmacologically target endogenous beta cells and activate GCK. So far, a number of synthetic compounds that influence GCK or its proposed activator 6PF2K/Fru2,6-P2ase have been successfully developed and evaluated, albeit without direct clinical potential [202]. Of course, our pseudoislet procedure can also be used to genetically engineer beta cells to make them express more (efficient) GCK. To identify more genes and pathways involved in the mechanisms behind beta cell adaptation, next generation sequencing technologies can be applied.

In a more distant future one could envision that our synthetic biology procedure becomes an integral part of the clinical islet transplantation process. To successfully cure diabetes, patients would be transplanted with tailor-made islets that are engineered to have a superior quality and survival, and resist immune-mediated attacks. In such a scheme, GPCRs and GCK are just two examples of candidate proteins that can be modulated to improve islet function.

In conclusion, using our newly established tools to assess and improve beta cell function *in vivo*, we were able to perform a comprehensive and unparalleled functional phenotyping of beta cells in the living organism. The technical innovations and biological mechanisms presented in this thesis contribute to greater efforts in the field of diabetes research aiming to advance diagnostics and therapeutics.

6 ACKNOWLEDGEMENTS

During the past five years, I have had the pleasure to meet and work with some wonderful people. It goes without saying that many of you have contributed to the great times I have had whilst working to finish this thesis. The following people deserve some special attention:

First and foremost, I would like to express my sincere gratitude to **Erwin**. It has been an incredible fortune and privilege to have had you as a supervisor. I have enjoyed every minute of our discussions, collaborations, travels, revisions, etcetera. Thank you so much for all your patience and the enormous help during the past years. You are without doubt an excellent researcher and I hope that I was a good first PhD student for you.

Per-Olof, my co-supervisor, it has been an honour to work in your lab. I acknowledge you for placing your trust and confidence in my abilities to do science. I am thankful for the valuable lessons in the lab and on the tennis court.

My incredible colleagues: **Andrea**, you were always willing to help me, with whatever and whenever I needed an extra pair of hands, making an invaluable contribution to my work. Thank you so much! **Karin**, thank you for showing me that there is more than work alone. For always being up for fika, ice cream, or lunch in the park. **Tomas**, the other part of this unique trinity, thanks for the unforgettable times in Stockholm and Umeå. I have missed you two a lot since you left. **Anya**, **Concha**, **Ismael**, **Stefan**, **Teresa P.** and **Yan**, you crazy bunch! I will miss your laughter, the nice coffee and lunch breaks, the (margarita-)dinners, and the fun we had during the scientific meetings. **Lars**, **Meike**, **Neil** and **Montse**, you were excellent office mates. **Essam**, thank you for your generosity with candy, beer and whiskey. **Anderson**, **Connla**, **Eduardo**, **Jantje**, **Fernando**, **Karen**, **Subu**, **Teresa D.**, **Thais** and **Yixin**, thanks for the great pubs, barbecues, and more. I know we will stay friends!

Other present and former colleagues at the Rolf Luft Research Center, including: **Barbara Cheng**, **Chris**, **Elisabetta**, **Irfan**, **Galyna**, **Ingo**, **Irina**, **Jia**, **Kaixuan**, **Lina**, **Lisa**, **Luo-Sheng**, **Max**, **Martin**, **Nancy**, **Noah**, **Saad**, **Sabrina**, **Sampath**, **Sergei**, **Shao-Nian**, **Sofie**, **Tilo**, **Thusita** and **Yue**; I would like to thank you, as well as our colleagues from Miami, Singapore and Pohang, for big and small contributions to my work.

For invaluable administrative, technical and animal support, I would like to acknowledge the following people: **Katarina**, **Yvonne**, **Monica**, **Ann-Britt**, **Kerstin**, **Britt-Marie**, **Jan-Erik**, **Thomas**, and all the staff from the core facilities.

My collaborators, it has been a pleasure working with you all. A special thanks to **Ulf**, for your hospitality during the time I got to spend in your lab in Umeå. **Chris**, **Josie**, **Max**, **Saba**, and particularly **Maria**, thank you for making my life in Umeå so much easier and more enjoyable. Other collaborators I would like to acknowledge include: **Robin**, **Robert** and **Craig**; **Helder**, **Yesi**, and **Anders**; **Sven**, **Ping**, **Åsa**, and **Rickard**.

During the first three years of my PhD time I participated in the E.U. funded BetaTrain project. I would like to thank all those involved for a fantastic time during our meetings. In particular, the other Marie Curie fellows (not yet mentioned): **Andrea**, **Filippo**, **Janne**, **Vineetha**, **Greg**, **Shweta**, **Sandeep**, **Rita**, **Romain**, **Selen**, **Stefanie** and **Wael**. I wish you all the best in your careers and hope our paths cross at some point in the future.

My amazing friends, with whom I explored the corners of Stockholm, Sweden and beyond, far away from the lab. I especially thank, amongst so many other things, you: **Shahul**, for letting me be part of your Stockholm family and offering perspective; **Jonathan**, for being a loyal friend in good and bad times; **Erik** for your endless optimism and for making me believe in myself; **Susi** for your honesty and hospitality, for (not) being one of the guys; **Fritzi,** for unforgettable concerts, parties and trips; **Anna,** for cultural and culinary enrichment; **Melissa,** for never bailing and always being the last (wo)man standing; **Frankie**, for teaching me I should be myself; **Helena** for always smiling and having the best students; **Fra**, for your perseverance and joyfulness; **Milena**, for giving me the best nickname; **Laila**, for not taking life too seriously and teaching me how to dab; **Juan**, for bad jokes and good after works; **Isa**, for your kindness and determination; And **all those other friends** I did not mention, it was a great pleasure getting to know you. Let's hope for more adventures to come!

My dear family, to whom I dedicate this thesis: my parents **Frits** and **Liesbeth,** and my siblings **Bram** and **Anne**. I have very much appreciated all your support throughout the years. Without it I would not have been where I am today. A special thanks to my mother for designing the cover of this thesis.

And last but not least my beloved partner **Henriette**. Thank you so much for always standing by my side even though – sometimes – you were far away, for you love and understanding, and for your dedication. You make me get the best out of myself, not only as a scientist but as a person.

7 REFERENCES

1. Hörnblad A, Cheddad A, Ahlgren U (2011) An improved protocol for optical projection tomography imaging reveals lobular heterogeneities in pancreatic islet and β-cell mass distribution. Islets 3:204–208.
2. Hara M, Dizon RF, Glick BS, et al (2006) Imaging Pancreatic β-cells in the Intact Pancreas. AJP: Endocrinology and Metabolism 290:E1041–7.
3. Alanentalo T, Hornblad A, Mayans S, et al (2010) Quantification and Three-Dimensional Imaging of the Insulitis-Induced Destruction of β-Cells in Murine Type 1 Diabetes. Diabetes 59:1756–1764.
4. Kim A, Miller K, Jo J, et al (2014) Islet architecture: A comparative study. Islets 1:129–136.
5. Brissova M (2005) Assessment of Human Pancreatic Islet Architecture and Composition by Laser Scanning Confocal Microscopy. Journal of Histochemistry and Cytochemistry 53:1087–1097.
6. Arrojo e Drigo R, Ali Y, Diez J, et al (2015) New insights into the architecture of the islet of Langerhans: a focused cross-species assessment. Diabetologia 58:2218–2228.
7. Cabrera O, Berman DM, Kenyon NS, et al (2006) The unique cytoarchitecture of human pancreatic islets has implications for islet cell function. Proceedings of the National Academy of Sciences 103:2334–2339.
8. Halban PA, Powers SL, George KL, Bonner-Weir S (1987) Spontaneous reassociation of dispersed adult rat pancreatic islet cells into aggregates with three-dimensional architecture typical of native islets. Diabetes 36:783–790.
9. Ballian N, Brunicardi FC (2007) Islet Vasculature as a Regulator of Endocrine Pancreas Function. World J Surg 31:705–714.
10. Smith PH, Davis BJ (1983) Morphological and Functional Aspects of Pancreatic-Islet Innervation. J Auton Nerv Syst 9:53–66.
11. Nyman LR, Ford E, Powers AC, Piston DW (2010) Glucose-dependent blood flow dynamics in murine pancreatic islets in vivo. AJP: Endocrinology and Metabolism 298:E807–E814.
12. Jansson L, Hellerstrom C (1986) Glucose-induced changes in pancreatic islet blood flow mediated by central nervous system. Am J Physiol Endocrinol Metab 251:E644–E647.
13. Short KW, Head WS, Piston DW (2014) Connexin 36 mediates blood cell flow in mouse pancreatic islets. AJP: Endocrinology and Metabolism 306:E324–E331.
14. Diez JA, Arrojo e Drigo R, Zheng X, et al (2017) Pancreatic Islet Blood Flow Dynamics in Primates. Cell Rep 20:1490–1501.
15. Rodriguez-Diaz R, Speier S, Molano RD, et al (2012) Noninvasive in vivo model demonstrating the effects of autonomic innervation on pancreatic islet function. Proc Natl Acad Sci USA 109:21456–21461.
16. Rodriguez-Diaz R, Abdulreda MH, Formoso AL, et al (2011) Innervation patterns of autonomic axons in the human endocrine pancreas. Cell Metabolism 14:45–54.
17. Rodriguez-Diaz R, Dando R, Jacques-Silva MC, et al (2011) Alpha cells secrete acetylcholine as a non-neuronal paracrine signal priming beta cell function in humans. Nat Med 17:888–892.
18. Dunn MF (2005) Zinc-ligand interactions modulate assembly and stability of the insulin hexamer - a review. Biometals 18:295–303.
19. Rorsman P, Renström E (2003) Insulin granule dynamics in pancreatic beta cells. Diabetologia 46:1029–1045.
20. Klemen MS, Dolenšek J, Rupnik MS, Stožer A (2017) The triggering pathway to insulin secretion: Functional similarities and differences between the human and the mouse β cells and their translational relevance. Islets 9:109–139.
21. Rorsman P, Braun M, Zhang Q (2011) Regulation of calcium in pancreatic α- and β-cells in health and disease. Cell Calcium 51:300–308.
22. Yang S-N, Shi Y, Yang G, et al (2014) Ionic mechanisms in pancreatic β cell signaling. Cell Mol Life Sci 71:4149–4177.

23. Lang DA, Matthews DR, Peto J, Turner RC (1979) Cyclic oscillations of basal plasma glucose and insulin concentrations in human beings. N Engl J Med 301:1023–1027.
24. Nunemaker CS, Wasserman DH, McGuinness OP, et al (2006) Insulin secretion in the conscious mouse is biphasic and pulsatile. AJP: Endocrinology and Metabolism 290:E523–9.
25. Kindmark H, Kohler M, Arkhammar P, et al (1994) Oscillations in cytoplasmic free calcium concentration in human pancreatic islets from subjects with normal and impaired glucose tolerance. Diabetologia 37:1121–1131.
26. Ahrén B (2009) Islet G protein-coupled receptors as potential targets for treatment of type 2 diabetes. Nat Rev Drug Discov 8:369–385.
27. Ravier MA, Güldenagel M, Charollais A, et al (2005) Loss of Connexin36 Channels Alters β-Cell Coupling, Islet Synchronization of Glucose-Induced Ca2+ and Insulin Oscillations, and Basal Insulin Release. Diabetes 54:1798–1807.
28. Speier S, Gjinovci A, Charollais A, et al (2007) Cx36-Mediated Coupling Reduces β-Cell Heterogeneity, Confines the Stimulating Glucose Concentration Range, and Affects Insulin Release Kinetics. Diabetes 56:1078–1086.
29. Johnston NR, Mitchell RK, Haythorne E, et al (2016) Beta Cell Hubs Dictate Pancreatic Islet Responses to Glucose. Cell Metabolism 24:389–401.
30. Halban PA, Wollheim CB, Blondel B, et al (1982) The Possible Importance of Contact between Pancreatic Islet Cells for the Control of Insulin Release. Endocrinology 111:86–94.
31. Head WS, Orseth ML, Nunemaker CS, et al (2012) Connexin-36 Gap Junctions Regulate In Vivo First- and Second-Phase Insulin Secretion Dynamics and Glucose Tolerance in the Conscious Mouse. Diabetes 61:1700–1707.
32. International Diabetes Federation (2017) IDF Diabetes Atlas 8th edition. Brussels, Belgium: International Diabetes Federation
33. Nalysnyk L, Hernandez-Medina M, Krishnarajah G (2010) Glycaemic variability and complications in patients with diabetes mellitus: evidence from a systematic review of the literature. Diabetes, Obesity and Metabolism 12:288–298.
34. Klinke DJ (2008) Extent of beta cell destruction is important but insufficient to predict the onset of type 1 diabetes mellitus. PLoS ONE 3:e1374.
35. Oram RA, Jones AG, Besser REJ, et al (2014) The majority of patients with long-duration type 1 diabetes are insulin microsecretors and have functioning beta cells. Diabetologia 57:187–191.
36. Vehik K, Dabelea D (2010) The changing epidemiology of type 1 diabetes: why is it going through the roof? Diabetes Metab Res Rev 27:3–13.
37. Eisenbarth GS (1986) Type I diabetes mellitus. A chronic autoimmune disease. N Engl J Med 314:1360–1368.
38. van Belle TL, Coppieters KT, Herrath von MG (2011) Type 1 diabetes: etiology, immunology, and therapeutic strategies. Physiol Rev 91:79–118.
39. Coppieters KT, Boettler T, Herrath von M (2012) Virus Infections in Type 1 Diabetes. Cold Spring Harb Perspect Med 2:a007682.
40. Vaarala O, Atkinson MA, Neu J (2008) The “perfect storm” for type 1 diabetes: the complex interplay between intestinal microbiota, gut permeability, and mucosal immunity. Diabetes 57:2555–2562.
41. King AJF (2012) The use of animal models in diabetes research. Br J Pharmacol 166:877–894.
42. Hanafusa T, Miyagawa J, Nakajima H, et al (1994) The NOD mouse. Diabetes Research and Clinical Practice 24:S307–S311.
43. Nakhooda AF, Like AA, Chappel CI, et al (1977) The spontaneously diabetic Wistar rat. Metabolic and morphologic studies. Diabetes 26:100–112.
44. Logothetopoulos J, Valiquette N, Madura E, Cvet D (1984) The Onset and Progression of Pancreatic Insulitis in the Overt, Spontaneously Diabetic, Young Adult BB Rat Studied by Pancreatic Biopsy. Diabetes 33:33–36.
45. Lenzen S (2007) The mechanisms of alloxan- and streptozotocin-induced diabetes. Diabetologia 51:216–226.

46. Thorel F, Népote V, Avril I, et al (2010) Conversion of adult pancreatic α-cells to β-cells after extreme β-cell loss. Nature 464:1149–1154.
47. Saito M, Iwawaki T, Taya C, et al (2001) Diphtheria toxin receptor-mediated conditional and targeted cell ablation in transgenic mice. Nat Biotechnol 19:746–750.
48. Kahn SE, Hull RL, Utzschneider KM (2006) Mechanisms linking obesity to insulin resistance and type 2 diabetes. Nature 444:840–846.
49. Talchai C, Lin HV, Kitamura T, Accili D (2009) Genetic and biochemical pathways of β-cell failure in type 2 diabetes. Diabetes, Obesity and Metabolism 11:38–45.
50. Rhodes CJ (2005) Type 2 diabetes-a matter of beta-cell life and death? Science 307:380–384.
51. Meier JJ, Bonadonna RC (2013) Role of reduced β-cell mass versus impaired β-cell function in the pathogenesis of type 2 diabetes. Diabetes Care 36 Suppl 2:S113–9.
52. Rahier J, Guiot Y, Goebbels RM, et al (2008) Pancreatic β-cell mass in European subjects with type 2 diabetes. Diabetes, Obesity and Metabolism 10:32–42.
53. Surwit RS, Kuhn CM, Cochrane C, et al (1988) Diet-Induced Type II Diabetes in C57BL/6J Mice. Diabetes 37:1163–1167.
54. Ingalls AM, Dickie MM, Snell GD (1950) Obese, a new mutation in the house mouse. J Hered 41:317–318.
55. Hummel KP, Dickie MM, Coleman DL (1966) Diabetes, a New Mutafton in the Mouse. Science 153:1127–1128.
56. Zucker LM, Antoniades HN (1972) Insulin and obesity in the Zucker genetically obese rat "fatty". Endocrinology 90:1320–1330.
57. Goto Y, Kakizaki M, Masaki N (1976) Production of Spontaneous Diabetic Rats by Repetition of Selective Breeding. Tohoku J Exp Med 119:85–90.
58. Khafagy E-S, Morishita M, Onuki Y, Takayama K (2007) Current challenges in non-invasive insulin delivery systems: A comparative review. Advanced Drug Delivery Reviews 59:1521–1546.
59. Unger RH, Cherrington AD (2012) Glucagonocentric restructuring of diabetes: a pathophysiologic and therapeutic makeover. J Clin Invest 122:4–12.
60. Nathan DM, Buse JB, Davidson MB, et al (2008) Medical Management of Hyperglycemia in Type 2 Diabetes: A Consensus Algorithm for the Initiation and Adjustment of Therapy: A consensus statement of the American Diabetes Association and the European Association for the Study of Diabetes. Diabetes Care 32:193–203.
61. Cerf ME (2013) Beta cell dynamics: beta cell replenishment, beta cell compensation and diabetes. Endocrine 44:303–311.
62. Migliorini A, Bader E, Lickert H (2014) Islet cell plasticity and regeneration. Molecular Metabolism 3:268–274.
63. De Groef S, Staels W, Van Gassen N, et al (2016) Sources of beta cells inside the pancreas. Diabetologia 59:1834–1837.
64. de Kort H, de Koning EJ, Rabelink TJ, et al (2011) Islet transplantation in type 1 diabetes. BMJ 342:d217.
65. Shapiro AM, Lakey JR, Ryan EA, et al (2000) Islet transplantation in seven patients with type 1 diabetes mellitus using a glucocorticoid-free immunosuppressive regimen. N Engl J Med 343:230–238.
66. Moore SJ, Gala-Lopez BL, Pepper AR, et al (2015) Bioengineered stem cells as an alternative for islet cell transplantation. World J Transplant 5:1–10.
67. Pagliuca FW, Millman JR, Gürtler M, et al (2014) Generation of functional human pancreatic β cells in vitro. Cell 159:428–439.
68. Merani S, Toso C, Emamaullee J, Shapiro AMJ (2008) Optimal implantation site for pancreatic islet transplantation. Br J Surg 95:1449–1461.
69. van der Windt DJ, Echeverri GJ, Ijzermans JNM, Cooper DKC (2008) The Choice of Anatomical Site for Islet Transplantation. Cell Transplant 17:1005–1014.

70. Jansson L, Carlsson PO (2002) Graft vascular function after transplantation of pancreatic islets. Diabetologia 45:749–763.
71. Speier S, Nyqvist D, Cabrera O, et al (2008) Noninvasive in vivo imaging of pancreatic islet cell biology. Nat Med 14:574–578.
72. Jones GL, Juszczak MT, Hughes SJ, et al (2007) Time course and quantification of pancreatic islet revascularizтion following intraportal transplantation. Cell Transplant 16:505–516.
73. Brissova M, Fowler M, Wiebe P, et al (2004) Intraislet endothelial cells contribute to revascularization of transplanted pancreatic islets. Diabetes 53:1318–1325.
74. Brissova M, Shostak A, Shiota M, et al (2006) Pancreatic Islet Production of Vascular Endothelial Growth Factor-A Is Essential for Islet Vascularization, Revascularization, and Function. Diabetes 55:2974–2985.
75. Nyqvist D, Köhler M, Wahlstedt H, Berggren P-O (2005) Donor Islet Endothelial Cells Participate in Formation of Functional Vessels Within Pancreatic Islet Grafts. Diabetes 54:2287–2293.
76. Davalli AM, Ogawa Y, Ricordi C, et al (1995) A selective decrease in the beta cell mass of human islets transplanted into diabetic nude mice. Transplantation 59:817–820.
77. Carlsson P-O, Palm F, Mattsson G (2002) Low revascularization of experimentally transplanted human pancreatic islets. J Clin Endocrinol Metab 87:5418–5423.
78. Lau J, Carlsson P-O (2009) Low revascularization of human islets when experimentally transplanted into the liver. Transplantation 87:322–325.
79. Bernard-Kargar C, Ktorza A (2001) Endocrine pancreas plasticity under physiological and pathological conditions. Diabetes 50 Suppl 1:S30–5.
80. Rieck S, Kaestner KH (2010) Expansion of beta-cell mass in response to pregnancy. Trends Endocrinol Metab 21:151–158.
81. Kassem SA, Ariel I, Thornton PS, et al (2000) Beta-cell proliferation and apoptosis in the developing normal human pancreas and in hyperinsulinism of infancy. Diabetes 49:1325–1333.
82. Finegood DT, Scaglia L, Bonner-Weir S (1995) Dynamics of beta-cell mass in the growing rat pancreas. Estimation with a simple mathematical model. Diabetes 44:249–256.
83. Teta M, Long SY, Wartschow LM, et al (2005) Very slow turnover of beta-cells in aged adult mice. Diabetes 54:2557–2567.
84. Brennand K, Melton D (2009) Slow and steady is the key to β-cell replication. Journal of Cellular and Molecular Medicine 13:472–487.
85. Pick A, Clark J, Kubstrup C, et al (1998) Role of apoptosis in failure of beta-cell mass compensation for insulin resistance and beta-cell defects in the male Zucker diabetic fatty rat. Diabetes 47:358–364.
86. Ilegems E, Dicker A, Speier S, et al (2013) Reporter islets in the eye reveal the plasticity of the endocrine pancreas. Proceedings of the National Academy of Sciences 110:20581–20586.
87. Dalbøge LS, Almholt DLC, Neerup TSR, et al (2013) Characterisation of age-dependent beta cell dynamics in the male db/db mice. PLoS ONE 8:e82813.
88. Sreenan S, Pick AJ, Levisetti M, et al (1999) Increased beta-cell proliferation and reduced mass before diabetes onset in the nonobese diabetic mouse. Diabetes 48:989–996.
89. Nir T, Melton DA, Dor Y (2007) Recovery from diabetes in mice by β cell regeneration. J Clin Invest 117:2553–2561.
90. Lee HC, Bonner-Weir S, Weir GC, Leahy JL (1989) Compensatory adaption to partial pancreatectomy in the rat. Endocrinology 124:1571–1575.
91. Tonne JM, Sakuma T, Munoz-Gomez M, et al (2014) Beta cell regeneration after single-round immunological destruction in a mouse model. Diabetologia 58:313–323.
92. Butler AE, Janson J, Bonner-Weir S, et al (2003) Beta-cell deficit and increased beta-cell apoptosis in humans with type 2 diabetes. Diabetes 52:102–110.
93. Butler AE, Galasso R, Meier JJ, et al (2007) Modestly increased beta cell apoptosis but no increased beta cell replication in recent-onset type 1 diabetic patients who died of diabetic ketoacidosis. Diabetologia 50:2323–2331.

94. Menge BA, Tannapfel A, Belyaev O, et al (2007) Partial Pancreatectomy in Adult Humans Does Not Provoke β-Cell Regeneration. Diabetes 57:142–149.
95. Stolovich-Rain M, Hija A, Grimsby J, et al (2012) Pancreatic beta cells in very old mice retain capacity for compensatory proliferation. J Biol Chem 287:27407–27414.
96. Rankin MM, Kushner JA (2009) Adaptive beta-cell proliferation is severely restricted with advanced age. Diabetes 58:1365–1372.
97. Kushner JA (2013) The role of aging upon β cell turnover. J Clin Invest 123:990–995.
98. Carlotti F, Zaldumbide A, Ellenbroek JH, et al (2011) β-Cell Generation: Can Rodent Studies Be Translated to Humans? Journal of Transplantation 2011:1–15.
99. Bonner-Weir S, Deery D, Leahy JL, Weir GC (1989) Compensatory growth of pancreatic beta-cells in adult rats after short-term glucose infusion. Diabetes 38:49–53.
100. Koiter TR, Wijkstra S, van der Schaaf-Verdonk CJ, et al (1995) Pancreatic beta-cell function and islet-cell proliferation: effect of hyperinsulinaemia. Physiol Behav 57:717–721.
101. Nollevaux MC, Rahier J, Marchandise J, et al (2013) Characterization of β-cell plasticity mechanisms induced in mice by a transient source of exogenous insulin. Am J Physiol Endocrinol Metab 304:E711–23.
102. Stamateris RE, Sharma RB, Kong Y, et al (2016) Glucose Induces Mouse β-Cell Proliferation via IRS2, MTOR, and Cyclin D2 but Not the Insulin Receptor. Diabetes 65:981–995.
103. Porat S, Weinberg-Corem N, Tornovsky-Babaey S, et al (2011) Control of pancreatic β cell regeneration by glucose metabolism. Cell Metabolism 13:440–449.
104. Ravier MA, Leduc M, Richard J, et al (2014) β-Arrestin2 plays a key role in the modulation of the pancreatic beta cell mass in mice. Diabetologia 57:532–541.
105. Davis DB, Lavine JA, Suhonen JI, et al (2010) FoxM1 is up-regulated by obesity and stimulates beta-cell proliferation. Mol Endocrinol 24:1822–1834.
106. Karnik SK, Chen H, McLean GW, et al (2007) Menin controls growth of pancreatic beta-cells in pregnant mice and promotes gestational diabetes mellitus. Science 318:806–809.
107. Kim H, Toyofuku Y, Lynn FC, et al (2010) Serotonin regulates pancreatic beta cell mass during pregnancy. Nat Med 16:804–808.
108. Szabat M, Lynn FC, Hoffman BG, et al (2012) Maintenance of β-cell maturity and plasticity in the adult pancreas: developmental biology concepts in adult physiology. Diabetes 61:1365–1371.
109. Aly H, Gottlieb P (2009) The honeymoon phase: intersection of metabolism and immunology. Current Opinion in Endocrinology, Diabetes and Obesity 16:286–292.
110. Martín F, Andreu E, Rovira JM, et al (1999) Mechanisms of glucose hypersensitivity in beta-cells from normoglycemic, partially pancreatectomized mice. Diabetes 48:1954–1961.
111. Peshavaria M, Larmie BL, Lausier J, et al (2006) Regulation of Pancreatic β-Cell Regeneration in the Normoglycemic 60% Partial-Pancreatectomy Mouse. Diabetes 55:3289–3298.
112. Roscioni SS, Migliorini A, Gegg M, Lickert H (2016) Impact of islet architecture on β-cell heterogeneity, plasticity and function. Nat Rev Endocrinol 12:695–709.
113. Pipeleers DG (1992) Heterogeneity in pancreatic beta-cell population. Diabetes 41:777–781.
114. Orci L (1974) A portrait of the pancreatic β-cell. Diabetologia 10:163–187.
115. Gonzalez A, Merino B, Marroquí L, et al (2013) Insulin Hypersecretion in Islets From Diet-Induced Hyperinsulinemic Obese Female Mice Is Associated With Several Functional Adaptations in Individual β-Cells. Endocrinology 154:3515–3524.
116. Wojtusciszyn A, Armanet M, Morel P, et al (2008) Insulin secretion from human beta cells is heterogeneous and dependent on cell-to-cell contacts. Diabetologia 51:1843–1852.
117. Jonkers FC, Henquin J-C (2001) Measurements of Cytoplasmic Ca2+ in Islet Cell Clusters Show That Glucose Rapidly Recruits β-Cells and Gradually Increases the Individual Cell Response. Diabetes 50:540–550.
118. Stefan Y, Meda P, Neufeld M, Orci L (1987) Stimulation of insulin secretion reveals heterogeneity of pancreatic B cells in vivo. J Clin Invest 80:175–183.

119. van der Meulen T, Mawla AM, DiGruccio MR, et al (2017) Virgin Beta Cells Persist throughout Life at a Neogenic Niche within Pancreatic Islets. Cell Metabolism 25:911–926.e6.
120. Dorrell C, Schug J, Canaday PS, et al (2016) Human islets contain four distinct subtypes of β cells. Nat Comms 7:11756.
121. Bader E, Migliorini A, Gegg M, et al (2016) Identification of proliferative and mature β-cells in the islets of Langerhans. Nature 535:430–434.
122. Ellenbroek JH, Töns HA, de Graaf N, et al (2013) Topologically Heterogeneous Beta Cell Adaptation in Response to High-Fat Diet in Mice. PLoS ONE 8:e56922–8.
123. Lau J, Svensson J, Grapensparr L, et al (2012) Superior beta cell proliferation, function and gene expression in a subpopulation of rat islets identified by high blood perfusion. Diabetologia 55:1390–1399.
124. Chen C, Chmelova H, Cohrs CM, et al (2016) Alterations in β-Cell Calcium Dynamics and Efficacy Outweigh Islet Mass Adaptation in Compensation of Insulin Resistance and Prediabetes Onset. Diabetes 65:2676–2685.
125. Irles E, Ñeco P, Lluesma M, et al (2015) Enhanced glucose-induced intracellular signaling promotes insulin hypersecretion: pancreatic beta-cell functional adaptations in a model of genetic obesity and prediabetes. Molecular and Cellular Endocrinology 404:46–55.
126. Do OH, Gunton JE, Gaisano HY, Thorn P (2016) Changes in beta cell function occur in prediabetes and early disease in the $Lepr^{db}$ mouse model of diabetes. Diabetologia 59:1222–1230.
127. Alarcon C, Boland BB, Uchizono Y, et al (2016) Pancreatic β-Cell Adaptive Plasticity in Obesity Increases Insulin Production but Adversely Affects Secretory Function. Diabetes 65:438–450.
128. Zhou YP, Cockburn BN, Pugh W, Polonsky KS (1999) Basal insulin hypersecretion in insulin-resistant Zucker diabetic and Zucker fatty rats: role of enhanced fuel metabolism. Metab Clin Exp 48:857–864.
129. Liu YQ, Jetton TL, Leahy JL (2002) Beta-cell adaptation to insulin resistance. Increased pyruvate carboxylase and malate-pyruvate shuttle activity in islets of nondiabetic Zucker fatty rats. Journal of Biological Chemistry 277:39163–39168.
130. Topp BG, Atkinson LL, Finegood DT (2007) Dynamics of insulin sensitivity, beta-cell function, and beta-cell mass during the development of diabetes in fa/fa rats. AJP: Endocrinology and Metabolism 293:E1730–5.
131. Liu YQ, Nevin PW, Leahy JL (2000) β-Cell adaptation in 60% pancreatectomy rats that preserves normoinsulinemia and normoglycemia. Am J Physiol Endocrinol Metab 279:E68–E73.
132. Leahy JL, Bumbalo LM, Chen C (1993) Beta-cell hypersensitivity for glucose precedes loss of glucose-induced insulin secretion in 90% pancreatectomized rats. Diabetologia 36:1238–1244.
133. Chen C, Hosokawa H, Bumbalo LM, Leahy JL (1994) Regulatory effects of glucose on the catalytic activity and cellular content of glucokinase in the pancreatic beta cell. Study using cultured rat islets. J Clin Invest 94:1616–1620.
134. Sorenson RL, Brelje TC, Hegre OD, et al (1987) Prolactin (in vitro) decreases the glucose stimulation threshold, enhances insulin secretion, and increases dye coupling among islet beta cells. Endocrinology 121:1447–1453.
135. Ohara-Imaizumi M, Kim H, Yoshida M, et al (2013) Serotonin regulates glucose-stimulated insulin secretion from pancreatic beta cells during pregnancy. Proceedings of the National Academy of Sciences 110:19420–19425.
136. Rieck S, White P, Schug J, et al (2009) The transcriptional response of the islet to pregnancy in mice. Mol Endocrinol 23:1702–1712.
137. Cersosimo E, Solis-Herrera C, Trautmann ME, et al (2014) Assessment of pancreatic β-cell function: review of methods and clinical applications. Curr Diabetes Rev 10:2–42.
138. Laurent D, Vinet L, Lamprianou S, et al (2015) Pancreatic β-cell imaging in humans: fiction or option? Diabetes, Obesity and Metabolism 18:6–15.
139. Sweet IR, Cook DL, Lernmark A, et al (2004) Non-invasive imaging of beta cell mass: a quantitative analysis. Diabetes Technol Ther 6:652–659.
140. Meier JJ (2008) Beta cell mass in diabetes: a realistic therapeutic target? Diabetologia 51:703–713.

141. Hutton JC, Davidson HW (2010) Getting beta all the time: discovery of reliable markers of beta cell mass. Diabetologia 53:1254–1257.
142. McCulloch DK, Koerker DJ, Kahn SE, et al (1991) Correlations of In Vivo β-Cell Function Tests With β-Cell Mass and Pancreatic Insulin Content in Streptozocin-Administered Baboons. Diabetes 40:673–679.
143. Larsen MO, Rolin B, Raun K, et al (2007) Evaluation of beta-cell mass and function in the Göttingen minipig. Diabetes, Obesity and Metabolism 9 Suppl 2:170–179.
144. Robertson RP (2007) Estimation of beta-cell mass by metabolic tests: necessary, but how sufficient? Diabetes 56:2420–2424.
145. Alanentalo T, Asayesh A, Morrison H, et al (2007) Tomographic molecular imaging and 3D quantification within adult mouse organs. Nat Meth 4:31–33.
146. Yang L, Ji W, Xue Y, Chen L (2013) Imaging beta-cell mass and function in situ and in vivo. J Mol Med 91:929–938.
147. Yamada K, Nakata M, Horimoto N, et al (2000) Measurement of glucose uptake and intracellular calcium concentration in single, living pancreatic beta-cells. Journal of Biological Chemistry 275:22278–22283.
148. Rutter GA, Tsuboi T, Ravier MA (2006) Ca2+ microdomains and the control of insulin secretion. Cell Calcium 40:539–551.
149. Zhao Y, Araki S, Wu J, et al (2011) An Expanded Palette of Genetically Encoded Ca2+ Indicators. Science 333:1888–1891.
150. Li D, Chen S, Bellomo EA, et al (2011) Imaging dynamic insulin release using a fluorescent zinc indicator for monitoring induced exocytotic release (ZIMIR). Proceedings of the National Academy of Sciences 108:21063–21068.
151. Tsuboi T, Rutter GA (2003) Insulin secretion by "kiss-and-run" exocytosis in clonal pancreatic islet beta-cells. Biochem Soc Trans 31:833–836.
152. Almaça J, Liang T, Gaisano HY, et al (2015) Spatial and temporal coordination of insulin granule exocytosis in intact human pancreatic islets. Diabetologia 58:2810–2818.
153. Malaisse WJ, Maedler K (2012) Imaging of the β-cells of the islets of Langerhans. Diabetes Research and Clinical Practice 98:11–18.
154. Moore A (2009) Advances in beta-cell imaging. European Journal of Radiology 70:254–257.
155. Virostko J, Radhika A, Poffenberger G, et al (2009) Bioluminescence Imaging in Mouse Models Quantifies β Cell Mass in the Pancreas and After Islet Transplantation. Mol Imaging Biol 12:42–53.
156. Coppieters K, Martinic MM, Kiosses WB, et al (2010) A Novel Technique for the In Vivo Imaging of Autoimmune Diabetes Development in the Pancreas by Two-Photon Microscopy. PLoS ONE 5:e15732.
157. Villiger M, Goulley J, Friedrich M, et al (2009) In vivo imaging of murine endocrine islets of Langerhans with extended-focus optical coherence microscopy. Diabetologia 52:1599–1607.
158. Nyman LR, Wells KS, Head WS, et al (2008) Real-time, multidimensional in vivo imaging used to investigate blood flow in mouse pancreatic islets. J Clin Invest 118:3790–3797.
159. Berclaz C, Szlag D, Nguyen D, et al (2016) Label-free fast 3D coherent imaging reveals pancreatic islet micro-vascularization and dynamic blood flow. Biomed Opt Express 7:4569–4580.
160. Ritsma L, Steller EJA, Beerling E, et al (2012) Intravital microscopy through an abdominal imaging window reveals a pre-micrometastasis stage during liver metastasis. Sci Transl Med 4:158ra145.
161. van Gurp L, Loomans CJM, van Krieken PP, et al (2016) Sequential intravital imaging reveals in vivo dynamics of pancreatic tissue transplanted under the kidney capsule in mice. Diabetologia 59:2387–2392.
162. Leibiger IB, Berggren P-O (2017) Intraocular in vivo imaging of pancreatic islet cell physiology/pathology. Molecular Metabolism 6:1002–1009.
163. Schmidt-Christensen A, Hansen L, Ilegems E, et al (2013) Imaging dynamics of CD11c+ cells and Foxp3+ cells in progressive autoimmune insulitis in the NOD mouse model of type 1 diabetes. Diabetologia 56:2669–2678.

164. Åvall K, Ali Y, Leibiger IB, et al (2015) Apolipoprotein CIII links islet insulin resistance to β-cell failure in diabetes. Proceedings of the National Academy of Sciences 112:E2611–E2619.
165. Nord C, Eriksson M, Dicker A, et al (2017) Biochemical profiling of diabetes disease progression by multivariate vibrational microspectroscopy of the pancreas. Sci Rep 7:6646.
166. Hara M, Wang X, Kawamura T, et al (2003) Transgenic mice with green fluorescent protein-labeled pancreatic β-cells. AJP: Endocrinology and Metabolism 284:E177–83.
167. Paschen M, Moede T, Leibiger B, et al (2016) Non-invasive cell type selective in vivo monitoring of insulin resistance dynamics. Sci Rep 6:21448.
168. Thorens B, Tarussio D, Maestro MA, et al (2014) Ins1cre knock-in mice for beta cell-specific gene recombination. Diabetologia 58:558–565.
169. Zariwala HA, Borghuis BG, Hoogland TM, et al (2012) A Cre-Dependent GCaMP3 Reporter Mouse for Neuronal Imaging In Vivo. J Neurosci 32:3131–3141.
170. Tian L, Hires SA, Mao T, et al (2009) Imaging neural activity in worms, flies and mice with improved GCaMP calcium indicators. Nat Meth 6:875–881.
171. Eriksson AU, Svensson C, Hörnblad A, et al (2013) Near infrared optical projection tomography for assessments of β-cell mass distribution in diabetes research. JoVE e50238.
172. Sharpe J (2002) Optical Projection Tomography as a Tool for 3D Microscopy and Gene Expression Studies. Science 296:541–545.
173. Ricordi C, Lacy PE, Finke EH, et al (1988) Automated method for isolation of human pancreatic islets. Diabetes 37:413–420.
174. Roe MW, Lemasters JJ, Herman B (1990) Assessment of Fura-2 for measurements of cytosolic free calcium. Cell Calcium 11:63–73.
175. Kindmark H, Kohler M, Efendić S, et al (1992) Protein kinase C activity affects glucose-induced oscillations in cytoplasmic free Ca2+ in the pancreatic β-cell. FEBS Lett 303:85–90.
176. Speier S, Nyqvist D, Köhler M, et al (2008) Noninvasive high-resolution in vivo imaging of cell biology in the anterior chamber of the mouse eye. Nat Protoc 3:1278–1286.
177. Skala M, Ramanujam N (2010) Multiphoton redox ratio imaging for metabolic monitoring in vivo. Methods Mol Biol 594:155–162.
178. Cheddad A, Svensson C, Sharpe J, et al (2012) Image Processing Assisted Algorithms for Optical Projection Tomography. IEEE Trans Med Imaging 31:1–15.
179. Schindelin J, Arganda-Carreras I, Frise E, et al (2012) Fiji: an open-source platform for biological-image analysis. Nat Meth 9:676–682.
180. Picelli S, Faridani OR, Björklund AK, et al (2014) Full-length RNA-seq from single cells using Smart-seq2. Nat Protoc 9:171–181.
181. Sabek O, Gaber MW, Wilson CM, et al (2010) Imaging of human islet vascularization using a dorsal window model. Transplantation Proceedings 42:2112–2114.
182. Alanentalo T, Asayesh A, Morrison H, et al (2007) Tomographic molecular imaging and 3D quantification within adult mouse organs. Nat Meth 4:31–33.
183. Köhler M, Daré E, Ali MY, et al (2012) One-step purification of functional human and rat pancreatic alpha cells. Integrative Biology 4:209–219.
184. Egger MD, Petrăn M (1967) New reflected-light microscope for viewing unstained brain and ganglion cells. Science 157:305–307.
185. Jacques SL (2013) Optical properties of biological tissues: a review. Phys Med Biol 58:R37–61.
186. Matveyenko AV, Butler PC (2008) Relationship between β-cell mass and diabetes onset. Diabetes, Obesity and Metabolism 10:23–31.
187. Hanley SC, Austin E, Assouline-Thomas B, et al (2010) β-Cell Mass Dynamics and Islet Cell Plasticity in Human Type 2 Diabetes. Endocrinology 151:1462–1472.
188. Akirav E, Kushner JA, Herold KC (2008) Beta-Cell Mass and Type 1 Diabetes: Going, Going, Gone? Diabetes 57:2883–2888.
189. Abdulreda MH, Faleo G, Molano RD, et al (2011) High-resolution, noninvasive longitudinal live imaging of immune responses. Proc Natl Acad Sci USA 108:12863–12868.

190. Virostko J, Henske J, Vinet L, et al (2011) Multimodal image coregistration and inducible selective cell ablation to evaluate imaging ligands. Proc Natl Acad Sci USA 108:20719–20724.
191. Yamaizumi M, Mekada E, Uchida T, Okada Y (1978) One Molecule of Diphtheria Toxin Fragment A Introduced into a Cell Can Kill the Cell. Cell 15:1–6.
192. Fujiwara Y, Hiroyama M, Sanbe A, et al (2007) Insulin hypersensitivity in mice lacking the V1b vasopressin receptor. The Journal of Physiology 584:235–244.
193. Oshikawa S, Tanoue A, Koshimizu T-A, et al (2004) Vasopressin stimulates insulin release from islet cells through V1b receptors: a combined pharmacological/knockout approach. Mol Pharmacol 65:623–629.
194. Caton D, Calabrese A, Mas C, et al (2003) Lentivirus-mediated transduction of connexin cDNAs shows level- and isoform-specific alterations in insulin secretion of primary pancreatic beta-cells. Journal of Cell Science 116:2285–2294.
195. Wojtusciszyn A, Armanet M, Morel P, et al (2008) Insulin secretion from human beta cells is heterogeneous and dependent on cell-to-cell contacts. Diabetologia 51:1843–1852.
196. Newsholme P, Krause M (2012) Nutritional regulation of insulin secretion: implications for diabetes. The Clinical Biochemist Reviews 33:35–47.
197. Mendola JF, Goity C, Fernández-Alvarez J, et al (1994) Immunocytochemical study of pancreatic islet revascularization in islet isograft. Transplantation 57:725–730.
198. Menger MD, Vajkoczy P, Leiderer R, et al (1992) Influence of experimental hyperglycemia on microvascular blood perfusion of pancreatic islet isografts. J Clin Invest 90:1361–1369.
199. Soria B, Martín F, Andreu E, et al (1996) Diminished fraction of blockable ATP-sensitive K+ channels in islets transplanted into diabetic mice. Diabetes 45:1755–1760.
200. Negi S, Jetha A, Aikin R, et al (2012) Analysis of Beta-Cell Gene Expression Reveals Inflammatory Signaling and Evidence of Dedifferentiation following Human Islet Isolation and Culture. PLoS ONE 7:e30415.
201. MacDonald PE, Joseph JW, Rorsman P (2005) Glucose-sensing mechanisms in pancreatic beta-cells. Philos Trans R Soc Lond, B, Biol Sci 360:2211–2225.
202. Matschinsky FM (2009) Assessing the potential of glucokinase activators in diabetes therapy. Nat Rev Drug Discov 8:399–416.
203. Gotthardt M, Eizirik DL, Cnop M, Brom M (2014) Beta cell imaging - a key tool in optimized diabetes prevention and treatment. Trends Endocrinol Metab 25:375–377.
204. Shishido A, Caicedo A, Rodriguez-Diaz R, Pileggi A (2016) Clinical intraocular islet transplantation is not a number issue. CellR 4:2120.
205. Kendall DM, Sutherland DE, Najarian JS, et al (1990) Effects of hemipancreatectomy on insulin secretion and glucose tolerance in healthy humans. N Engl J Med 322:898–903.
206. Xu G, Kaneto H, Laybutt DR, et al (2007) Downregulation of GLP-1 and GIP Receptor Expression by Hyperglycemia: Possible Contribution to Impaired Incretin Effects in Diabetes. Diabetes 56:1551–1558.
207. Dunér P, Al-Amily IM, Soni A, et al (2016) Adhesion G Protein-Coupled Receptor G1 (ADGRG1/GPR56) and Pancreatic β-Cell Function. J Clin Endocrinol Metab 101:4637–4645.
208. Guettier J-M, Gautam D, Scarselli M, et al (2009) A chemical-genetic approach to study G protein regulation of beta cell function in vivo. Proc Natl Acad Sci USA 106:19197–19202.